Sutoh, K., & Lu, R. C. (1987) *Biochemistry 26*, 4511–4516.
Sutoh, K., Yamamoto, K., & Wakabayashi, T. (1984) *J. Mol. Biol. 178*, 323–339.
Sutoh, K., Yamamoto, K., & Wakabayashi, T. (1986) *Proc. Natl. Acad. Sci. U.S.A. 83*, 212–216.
Sutoh, K., Tokunaga, M., & Wakabayashi, T. (1987) *J. Mol. Biol. 195*, 953–956.
Szilagi, L., Balint, M., Stretrer, F. A., & Gergely, J. (1979) *Biochem. Biophys. Res. Commun. 87*, 936–945.
Tao, T., & Lamkin, M. (1981) *Biochemistry 20*, 5051–5055.
Tokunaga, M., Sutoh, K., Toyoshima, C., & Wakabayashi, T. (1987) *Nature (London) 329*, 635–638.
Tong, S. W., & Elzinga, M. (1983) *J. Biol. Chem. 258*, 13100–13110.
Towbin, H. M., Staehelin, T. M., & Gordon, J. (1979) *Proc. Natl. Acad. Sci. U.S.A. 76*, 4350–4354.
Vanaman, T. C., & Stark, G. R. (1970) *J. Biol. Chem. 245*, 3565–3573.
Walker, J. E., Saraste, M., Runswick, M. J., & Gay, N. J. (1982) *EMBO J. 1*, 945–951.
Warrick, H. M., De Lozanne, A., Leinwand, L. A., & Spudich, J. A. (1986) *Proc. Natl. Acad. Sci. U.S.A. 83*, 9433–9437.
Weeds, A. G., & Taylor, R. S. (1975) *Nature (London) 257*, 54–56.
Yount, R. G., Okamoto, Y., Mahmood, R., & Grammer, J. (1985) Abstracts of the 11th Yamada Conference, Kobe, Japan, Aug 1985, p 41.

Reactions of the Sarcoplasmic Reticulum Calcium Adenosinetriphosphatase with Adenosine 5′-Triphosphate and Ca^{2+} That Are Not Satisfactorily Described by an E_1–E_2 Model†

Neil Stahl and William P. Jencks*
Graduate Department of Biochemistry, Brandeis University, Waltham, Massachusetts 02254
Received April 1, 1987; Revised Manuscript Received July 7, 1987

ABSTRACT: Phosphorylation of the sarcoplasmic reticulum calcium ATPase, E, is first order with k_b = 70 ± 7 s^{-1} after free enzyme was mixed with saturating ATP and 50 μM Ca^{2+}; this is one-third the rate constant of 220 s^{-1} for phosphorylation of enzyme preincubated with calcium, $^cE{\cdot}Ca_2$, after being mixed with ATP under the same conditions (pH 7.0, Ca^{2+}-loaded vesicles, 100 mM KCl, 5 mM Mg^{2+}, 25 °C). Phosphorylation of E with ATP and Ca^{2+} in the presence of 0.25 mM ADP gives ~50% $E{\sim}P{\cdot}Ca_2$ with k_{obsd} = 77 s^{-1}, not the sum of the forward and reverse rate constants, $k_{obsd} = k_f + k_r$ = 140 s^{-1}, that is expected for approach to equilibrium if phosphorylation were rate limiting. These results show that (1) k_b represents a slow conformational change, rather than phosphoryl transfer, and (2) different pathways are followed for the phosphorylation of E and of $^cE{\cdot}Ca_2$. The absence of a lag for phosphorylation of E with saturating ATP and Ca^{2+} indicates that all other steps, including the binding of Ca^{2+} ions and phosphoryl transfer, have rate constants of >500 s^{-1}. Chase experiments with unlabeled ATP or with ethylene glycol bis(β-aminoethyl ether)-*N*,*N*,*N*′,*N*′-tetraacetic acid (EGTA) show that the rate constants for dissociation of [γ-^{32}P]ATP and Ca^{2+} are comparable to k_b. Dissociation of ATP occurs at 47 s^{-1} from $E{\cdot}ATP{\cdot}Ca^{2+}$ and at 24 s^{-1} from E·ATP. Approximately 20% phosphorylation occurs following an EGTA chase 4.5 ms after the addition of 300 μM ATP and 50 μM Ca^{2+} to enzyme. This shows that Ca^{2+} binds rapidly to the free enzyme, from outside the vesicle, before the conformational change (k_b). The fraction of Ca^{2+}-free E·[γ-^{32}P]ATP that is trapped to give labeled phosphoenzyme after the addition of Ca^{2+} and a chase of unlabeled ATP is half-maximal at 6.8 μM Ca^{2+}, with a Hill slope of n = 1.8. The calculated dissociation constant for Ca^{2+} from $E{\cdot}ATP{\cdot}Ca_2$ is ~2.2 × 10^{-10} M^2 ($K_{0.5}$ = 15 μM). The rate constant for the slow phase of the biphasic reaction of $E{\sim}P{\cdot}Ca_2$ with 1.1 mM ADP increases 2.5-fold when [Ca^{2+}] is decreased from 50 μM to 10 nM, with half-maximal increase at 1.7 μM Ca^{2+}. This shows that Ca^{2+} is dissociating from a different species, $^aE{\cdot}ATP{\cdot}Ca_2$, that is active for catalysis of phosphoryl transfer, has a high affinity for Ca^{2+}, and dissociates Ca^{2+} with $k \leq$ 45 s^{-1}. It is concluded that steady-state turnover of the ATPase under most conditions occurs through the $E{\cdot}ATP{\cdot}Ca_2$ pathway, which has a relatively low affinity for Ca^{2+}, not the pathway through $^cE{\cdot}Ca_2$ (or "$E_1{\cdot}Ca_2$"). This results in 11–17% unphosphorylated enzyme in the steady state at saturating [ATP] and [Ca^{2+}] because the k_b step is partly rate limiting. The two pathways for phosphorylation can result in nonlinear Lineweaver–Burk plots for ATP and initial overshoots of phosphoenzyme levels.

Reactions of the calcium ATPase (E)[1] of sarcoplasmic reticulum with its substrates ATP and Ca^{2+} can occur by two pathways, depending on the concentrations of ATP and Ca^{2+}. The upper pathway in eq 1 is the well-known pathway in which calcium binds first and causes a conformational change before

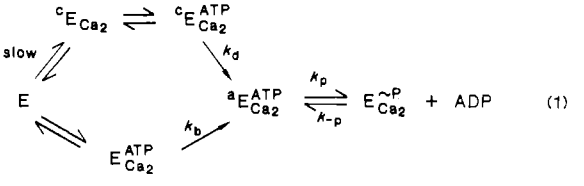

(1)

phosphorylation by ATP; the initial product of this reaction is designated $^cE{\cdot}Ca_2$ simply to indicate that it is the stable form

† This is Publication No. 1614. This research was supported in part by grants from the National Institutes of Health (GM20888) and the National Science Foundation (PCM-8117816).

0006-2960/87/0426-7654$01.50/0

Scheme I

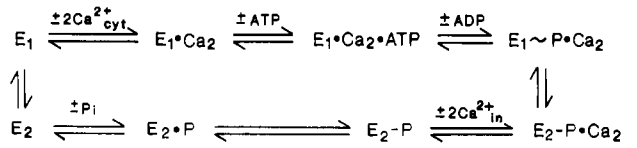

of the enzyme with bound calcium. Binding of ATP to $^{c}E{\cdot}Ca_2$ causes a second conformational change, with a rate constant of $k_d = 220\ s^{-1}$, which converts the enzyme to a catalytically active form, $^{a}E{\cdot}Ca_2{\cdot}ATP$, that is phosphorylated very rapidly with a rate constant of $k_p \geq 1000\ s^{-1}$ (Petithory & Jencks, 1986).

The lower pathway in eq 1 is followed when ATP binds first or ATP and calcium are added together to the enzyme. We describe here the properties of this pathway, which are quite different from those of the upper pathway. It is almost certainly the pathway that is followed in vivo, where the ATP concentration is well above millimolar (Veech et al., 1979) and the calcium concentration changes from less than 0.1 μM to the micromolar range during muscle contraction (Tanford, 1981).

It is well-known that ATP increases the rate of a conformational change associated with calcium binding (Sumida et al., 1978; Takisawa & Tonomura, 1978; Scofano et al., 1979; Inesi et al., 1980; Guillain et al., 1981; Pickart & Jencks, 1984; Fernandez-Belda et al., 1984). It has been shown that this activation involves ATP that is bound to the catalytic site and phosphorylates the enzyme with a rate constant of 70 s^{-1} upon addition of calcium; there is evidence suggesting that this rate constant represents a conformational change (Stahl & Jencks, 1984). Similar behavior has been observed with bullfrog sarcoplasmic reticulum by Ogawa and Harafuji (1986), and a model for ATP activation has been proposed by these workers that has similarities, but also significant differences, compared with the model proposed by us. The results reported here provide further support for the assignment of this conformational change to the k_b step in the lower pathway of eq 1.

Models are essential for developing an understanding of complex systems such as the Ca and the Na,K-transporting ATPases, and the E_1–E_2 model shown in Scheme I (and the similar E–E* and the E–E′ models) has played an important role in the development of our present understanding of the mechanism of these enzymes (de Meis & Vianna, 1979; Siegel & Albers, 1967; Post et al., 1969; Glynn & Karlish, 1975). However, models have a tendency to take on a life of their own and may be mistaken for reality; this can impede understanding. Furthermore, the properties of the intermediates in these models are not always clearly defined, and some of them have never been observed. The results reported here and other data in the literature are not easily described by the E_1–E_2 model. We suggest that the properties of these enzymes should be described by a notation that is based simply on the chemical composition or a single, defined activity of the different enzyme forms.

Materials and Methods

Materials. Reagents were generally of the highest purity available and were used without further purification. Na_2ATP was obtained from Boehringer Mannheim (Sonderqualitat), and [γ-^{32}P]ATP (>98% purity) was purchased from New England Nuclear.

Tightly sealed sarcoplasmic reticulum vesicles were prepared from rabbit skeletal muscle by a slight modification of the MacLennan procedure, as described previously (Pickart & Jencks, 1982). The preparations hydrolyzed ATP at 3–5 μmol (mg of total protein)$^{-1}$ min^{-1} under the standard conditions described below when the vesicles were made permeable to calcium ions with 4 μg/mL of the calcium ionophore A23187. The total amount of phosphoenzyme, [E_{tot}], that was observed for intact vesicles with saturating [Ca^{2+}] and [ATP] was 2–3 nmol/mg total protein.

Methods. All experiments were performed at pH 7.0, 0.1 M KCl, 5 mM $MgSO_4$, and 25 °C unless otherwise noted. Ca-ATPase activity was assayed spectrophotometrically by coupling ADP production to NADH oxidation with pyruvate kinase and lactate dehydrogenase (Rossi et al., 1979). Standard conditions were 40 mM MOPS, 100 mM KCl, 5 mM $MgSO_4$, 0.41 mM $CaCl_2$, 0.40 mM EGTA (23 μM free Ca^{2+}), 1.5 mM ATP, pH 7.0, and 25 °C. Protein concentrations were determined by the procedure of Lowry et al. (1951), with bovine serum albumin as standard.

Concentrations of free calcium were calculated from a dissociation constant of $K_{diss} = 7.4 \times 10^{-7}$ M for Ca·EGTA (Godt, 1974). This value was chosen because it was measured directly under conditions of pH, [KCl], and [Mg^{2+}] identical with ours. It is nearly 4 times larger than the value of 2.0×10^{-7} M derived from the constants of Schwarzenbach (Schwarzenbach et al., 1957) and is up to twofold larger than some values used in the literature (Guillain et al., 1980; Ogawa, 1968; Allen, 1977). Therefore, it is necessary to divide the [Ca^{2+}] in this work by 4 or ~2 for comparison with results obtained from the smaller values of K_{diss}. The free Ca^{2+} concentrations were not corrected for the calculated changes resulting from changes in ATP concentration because these changes are smaller than the estimated error of the experimental data. The release of protons from EGTA upon formation of the Ca·EGTA complex was neutralized with 1.47 equiv of KOH added with the Ca^{2+} when high concentrations of Ca^{2+} and EGTA were mixed.

The formation or decay of phosphoenzyme was followed with a rapid-mixing apparatus that can be used with either three or four syringes of equal volume, as described previously (Stahl & Jencks, 1984). For three-syringe experiments, the temperature-equilibrated contents of syringes A and B are forced through a mixing block connected to a length of narrow-bore Teflon tubing for a time t_1 before being quenched in a second mixing block with hydrochloric acid from syringe C. For four-syringe experiments, another reactant pushed from syringe C is allowed to react for a time t_2 before being quenched with acid from syringe D in an additional mixing block. The quench solution contained 1.5 M HCl and 40 mM KH_2PO_4 for three-syringe experiments or 2 mM HCl and 55 mM KH_2PO_4 for four-syringe experiments. The reaction times were calibrated from measurements of the hydrolysis of 2,4-dinitrophenyl acetate by hydroxide ion (Barman & Gutfreund, 1964).

Measurement of [^{32}P]$E{\sim}P{\cdot}Ca_2$. Bovine serum albumin was added to the quenched reaction mixtures (0.30 mg/mL final concentration), followed by trichloroacetic acid at a final concentration of 12%, and the amount of [^{32}P]$E{\sim}P{\cdot}Ca_2$ was determined essentially as described by Verjovski-Almeida et al. (1978).

Passively Loaded SRV. Passively loaded SRV were used in some experiments in order to inhibit the hydrolysis of phosphoenzyme and permit accurate end-point determinations

[1] Abbreviations: SR, sarcoplasmic reticulum; SRV, sarcoplasmic reticulum vesicles; E, calcium adenosinetriphosphatase; EGTA, ethylene glycol bis(β-aminoethyl ether)-*N*,*N*,*N*′,*N*′-tetraacetic acid; MOPS, 4-morpholinepropanesulfonic acid; ATP*, [γ-^{32}P]ATP; PEP, phosphoenolpyruvate; Tris, tris(hydroxymethyl)aminomethane.

Scheme II

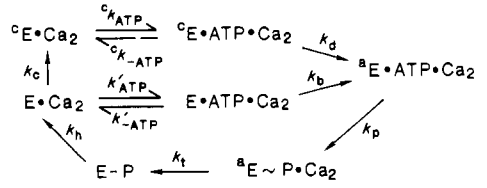

in the presence of a nonradioactive ATP chase. SRV were passively loaded with Ca^{2+} by incubation for 4–16 h at 4 °C in a solution containing 13–60 mg/mL SRV, 0.1 M KCl, 5 mM $MgSO_4$, 5 mM MOPS, pH 7.0, 0.32 M sucrose, and 20 mM $CaCl_2$, unless indicated otherwise. For each reaction, 10 μL of this stock solution was diluted into 0.99 mL of the reaction solution described for syringe A. This solution was loaded into syringe A of the rapid mixer, and the reaction was started within 15 s. This procedure results in the addition of 0.2 mM $CaCl_2$ in the A syringe.

Leaky Vesicles. SRV were made permeable to Ca^{2+} by incubation at room temperature in the presence of 118 mM Tris (pH 9.0–9.5) and 1 mM EGTA. The length of time required to achieve leakiness varied with different enzyme preparations and the concentration of SRV. Vesicles were judged to be leaky when the addition of A23187 to the standard assay failed to cause a rate increase. The leaky SRV were neutralized to pH ~7 with aqueous maleic acid. Typically, 1 mM Ca^{2+} was added to help stabilize the leaky enzyme. Leaky SRV stored on ice showed no evidence of becoming resealed with time.

Simulations. Simulations of the pre-steady-state kinetics were calculated with a program written for IBM-compatible microcomputers that allows input of rate or equilibrium expressions and the initial concentrations of each species for any model. The time course of a reaction is simulated by iterative calculation of the changes in the concentrations of each species over very small time increments, usually ≤1 μs. The time increment used in the simulation of a model was $\leq 0.01k^{-1}$, where k is the fastest rate constant in the model. The results can be shown on a graph or fit by a nonlinear least-squares procedure for estimation of rate constants.

Rate Equation for Scheme II at Saturating $[Ca^{2+}]$. A rate equation used for the simulation of Scheme II at saturating $[Ca^{2+}]$ was derived by Cleland's method of net rate constants (Cleland, 1975). Scheme II describes the reaction sequence at saturating $[Ca^{2+}]$ because the second-order binding of Ca^{2+} is rapid. The net rate constant for a reversible step is calculated from the rate constant for formation of the intermediate multiplied by the fraction of the intermediate that partitions forward. This fraction is equal to the rate constant for that step divided by the sum of the rate constants for every pathway through which the intermediate can decay. The velocity at a given enzyme concentration, $v/[E_{tot}]$, is equal to the reciprocal of the sums of the reciprocals for every net rate constant in the pathway. The velocity at each substrate concentration was calculated with a computer program from the expressions for the net rate constants shown below, the rate constants in Table II, and estimated values of ${}^{c}k_{ATP} = 10^7\ M^{-1}\ s^{-1}$ and $k'_{ATP} = 5.3 \times 10^6\ M^{-1}\ s^{-1}$.

The net rate constants for reversible steps are designated by the variable N:

$$ {}^{c}N_{ATP} = \frac{{}^{c}k_{ATP}[ATP]k_d}{k_d + {}^{c}k_{-ATP}} $$

$$ N'_{ATP} = \frac{k'_{ATP}[ATP]k_b}{k_b + k'_{-ATP}} $$

Scheme III

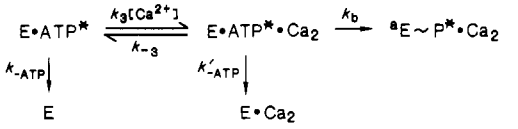

The term N_B is the net rate constant through the branched pathway for the disappearance of $E{\cdot}Ca_2$:

$$ N_B = \frac{k_c + N'_{ATP}}{1 + k_c/{}^{c}N_{ATP} + k_c/k_d + N'_{ATP}/k_b} $$

The velocity at a given enzyme concentration was calculated from

$$ v/[E_{tot}] = \frac{1}{1/k_p + 1/k_t + 1/k_h + 1/N_B} $$

Equation for Trapping E·ATP. The dependence on $[Ca^{2+}]$ of the fraction of E·ATP* trapped in a pulse–chase experiment, in which unlabeled ATP and calcium are added to E·ATP*, may be calculated according to Scheme III. A computer program that minimizes the sums of the squares of the residuals was used to obtain k_3, k_{-3}, and k'_{-ATP} from the equations shown below. The other rate constants are taken from Table II.

The net rate constant for the reversible step in this scheme is

$$ N_3 = \frac{k_3[Ca^{2+}]^2(k'_{-ATP} + k_b)}{k_b + k'_{-ATP} + k_{-3}} $$

The fraction trapped F_t can be calculated from the product of the fractions partitioning toward formation of phosphoenzyme at each step:

$$ F_t = \frac{N_3}{N_3 + k_{-ATP}} \frac{k_b}{k_b + k'_{-ATP}} $$

Results

Phosphorylation after Preincubation with EGTA. Figure 1 shows that the formation of $[^{32}P]E{\sim}P{\cdot}Ca_2$ occurs with an observed rate constant of 62 s^{-1} if passively loaded SRV are preincubated with EGTA for 15 s before mixing with 200 μM [γ-^{32}P]ATP and 50 mM Ca^{2+} (dotted line). An equally good fit is obtained with two consecutive first-order rate constants of 67 s^{-1} and 1060 s^{-1} (solid line; see below). An experiment similar to that shown in Figure 1 but with leaky vesicles, 100 μM Ca^{2+}, and 200 μM ATP gave the same initial rate of phosphorylation but a larger first-order rate constant of 84 s^{-1} for approach to the steady-state concentration of phosphoenzyme (not shown). This rate constant is the sum of the first-order rate constants for the formation and disappearance of phosphenzyme (Hiromi, 1979).

A similar rate constant of 77 s^{-1} is observed for phosphorylation to reach equilibrium in the presence of 0.25 mM ADP and 0.5–1.0 mM [γ-^{32}P]ATP with passively loaded SRV (Figure 2, solid lines). At these concentrations of ADP and ATP, the equilibrium amount of $E{\sim}P{\cdot}Ca_2$ formed is 0.46–0.53 of that observed in the absence of ADP.

Preincubation with the calcium ionophore A23187 results in a 24–30% decrease in the steady-state level of $[^{32}P]E{\sim}P{\cdot}Ca_2$ when passively loaded SRV react with 200 μM [γ-^{32}P]ATP and 100 μM Ca^{2+} for 2 s (Table I). The magnitude of the decrease is independent of the amount of ionophore added over a fourfold range. This decrease in the steady-state concentration of $[^{32}P]E{\sim}P{\cdot}Ca_2$ cannot be explained by the buildup of ADP because the addition of 9 μM ADP, which is an upper limit for the amount that can be formed in 2 s (calculated from

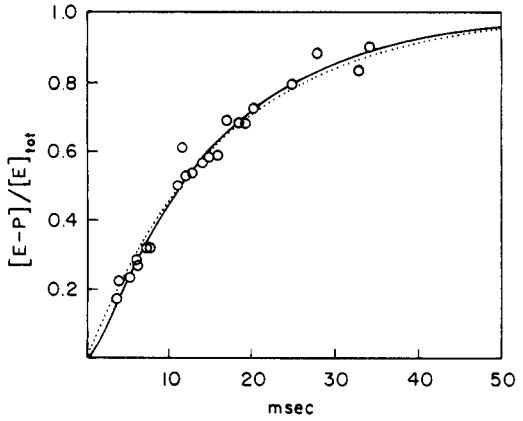

FIGURE 1: Formation of E∼P·Ca_2 by reaction of E with 200 μM [γ-^{32}P]ATP and 50 μM Ca^{2+}. Final conditions were 40 mM MOPS (pH 7.0), 100 mM KCl, 5 mM $MgSO_4$, 2.5 mM EGTA, 2.41 mM $CaCl_2$ (50 μM free calcium), 200 μM [γ-^{32}P]ATP, and 0.065 mg/mL SR protein at 25 °C. Syringe A contained 5.0 mM EGTA and 0.13 mg/mL SR protein; syringe B contained 4.82 mM $CaCl_2$ and 400 μM [γ-^{32}P]ATP; syringe C contained 1.5 N HCl and 40 mM KH_2PO_4. Other components were present in all syringes except C at their final concentrations. SRV were passively loaded with Ca^{2+} as described under Methods. A zero time point was measured by reversing the order of addition of syringes B and C. The best fit to a single exponential has a rate constant of 62 s^{-1} (dotted line). The solid line is calculated for two consecutive exponentials with rate constants of 67 s^{-1} and 1060 s^{-1}.

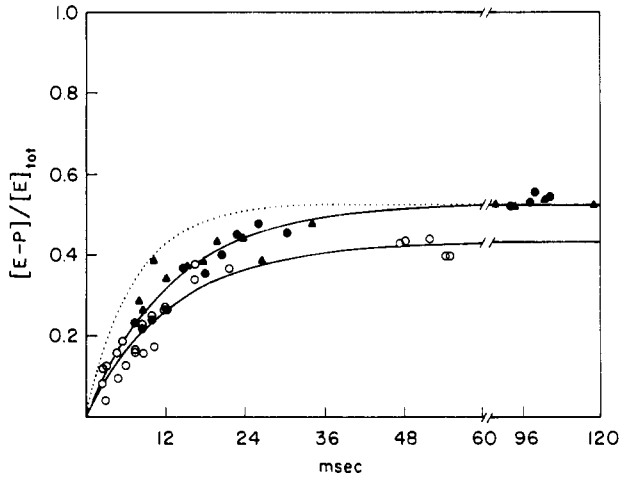

FIGURE 2: Phosphorylation of E to give E∼P·Ca_2 with 0.5 (○), 0.8 (●), and 1.0 (▲) mM ATP in the presence of 0.25 mM ADP. Conditions as in Figure 1 except syringe A contained 0.13, 0.27, or 0.27 mg/mL SR protein and syringe B contained 1.0, 1.6, or 2.0 mM [γ-^{32}P]ATP and 0.5 mM ADP. The solid lines are drawn for first-order reactions with a rate constant of 77 s^{-1} and end points of 0.46[E_{tot}] or 0.53[E_{tot}], while the dotted line is drawn for a rate constant of 140 s^{-1}.

the measured ATPase activity at 1 mM ATP) accounts for only half of the observed decrease (Table I). We conclude that at least 11–17% of the enzyme is unphosphorylated during steady-state turnover in the presence of 100 μM Ca^{2+} and 200 μM ATP.

*Trapping of E·ATP**. When passively loaded SRV were preincubated for 15 s with [γ-^{32}P]ATP and EGTA, followed by the addition of 50 μM Ca^{2+} and a chase of nonradioactive ATP, about 55% of the E∼P·Ca_2 formed contains ^{32}P (Figure 3, closed circles). The initial rates are the same, but the rate constant observed for phosphorylation in the presence of the nonradioactive ATP chase is 117 s^{-1} (closed circles), compared with 70 s^{-1} in the absence of the ATP chase (open circles). These results show that the rates of phosphorylation and dissociation of Ca^{2+} from E·ATP·Ca_2 are comparable.

Table I: Amount of E∼P·Ca_2 Observed in the Presence and Absence of the Ionophore A23187[a]

additions	[E–P]/[E_{tot}]	additions	[E–P]/[E_{tot}]
none	(1.0)	A23187 (49 mg/mL)	0.76
9 μM ADP	0.87	A23187 (25 mg/mL)	0.70
DMSO only	1.0	A23187 (12 mg/mL)	0.73

[a] Final conditions were 0.1 M KCl, 40 mM MOPS (pH 7.0), 5 mM $MgSO_4$, 200 μM [γ-^{32}P]ATP, and 100 μM Ca^{2+}. One milliliter of a solution containing 0.3 mg of passively loaded SRV, 0.1 M KCl, 40 mM MOPS (pH 7.0), 5 mM $MgSO_4$, 1 mM EGTA, and 1.1 mM $CaCl_2$ was incubated with the indicated additions for 15 s. Then, the reaction was started while vortexing by the addition of 1 mL of a solution containing 400 μM [γ-^{32}P]ATP, 1 mM EGTA, 1.1 mM $CaCl_2$, 0.1 M KCl, 40 mM MOPS (pH 7.0), and 5 mM $MgSO_4$, followed by the standard quench solution after 2 s. The volumes of the indicated additions were 5 μL of a 3.6 mM ADP solution and 2 μL for the DMSO or DMSO + A23187 solutions. The concentration indicated in the table is that for the stock A23187 solutions made in DMSO. The amount of E_{tot}, 2 nmol/mg, was taken from the amount of [^{32}P]E∼P·Ca_2 in the absence of any additions.

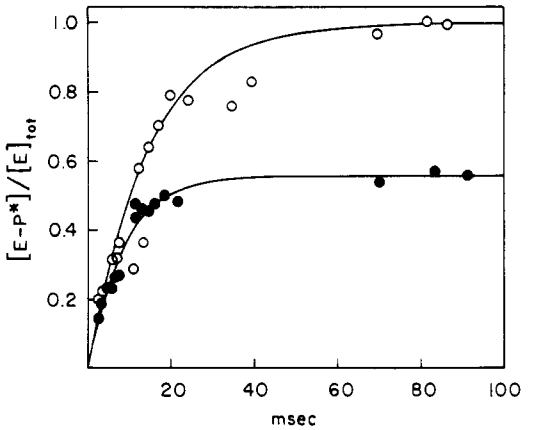

FIGURE 3: Formation of E∼P*·Ca_2 from E·ATP* with 50 μM Ca^{2+} in the presence of a nonradioactive ATP chase. Final conditions were 40 mM MOPS (pH 7.0), 100 mM KCl, 5 mM $MgSO_4$, 2.5 mM EGTA, 2.41 mM $CaCl_2$, 150 (○) or 30 μM (●) ATP, and 0.065 mg/mL SR protein at 25 °C. Syringe A contained 5.0 mM EGTA, 300 (○) or 60 μM (●) [γ-^{32}P]ATP, and 0.13 mg/mL passively loaded SR protein; syringe B contained 4.82 mM $CaCl_2$ and for the points marked (●) 2 mM nonradioactive ATP, 500 μM PEP, and 0.1 mg/mL pyruvate kinase. Syringe C contained 1.5 N HCl and 40 mM KH_2PO_4. Other components were present in all syringes except C at their final concentrations. The regenerating system in syringe B is required to remove ADP contamination from the ATP used as a chase. The points marked (○) are from Figure 1 of Stahl and Jencks (1984). The line drawn through the closed circles is for a first-order reaction with a rate constant of 117 s^{-1} and an end point of 0.56[E_{tot}].

The fraction of E·ATP* trapped decreases as the concentration of free Ca^{2+} in the ATP chase is lowered (Figure 4). Passively filled SRV were mixed with 15 μM [γ-^{32}P]ATP in the presence of 5 mM Mg^{2+} and 2 mM EGTA for 100–120 ms to form E·ATP* and then mixed with 0.5 mM nonradioactive ATP and various concentrations of free Ca^{2+} for ≥60 ms to allow phosphorylation to reach completion. Trapping of E·ATP* is half-maximal at 6.8 μM Ca^{2+}, and a Hill plot of the fraction trapped against Ca^{2+} concentration has a slope of 1.8 (Figure 4, inset). The line drawn through the points of Figure 4 was calculated from the equations describing trapping for Scheme III (Materials and Methods).

The dissociation of [γ-^{32}P]ATP from E·ATP* occurs with a rate constant of 24 s^{-1} in the presence of 5 mM Mg^{2+} (Figure 5). This was measured with the four-syringe mixing apparatus by preincubating passively loaded SRV with 15 μM [γ-^{32}P]-ATP in the presence of 5 mM EGTA and 5 mM Mg^{2+} for 15 s to form E·ATP*, then mixing with an excess of unlabeled ATP in the absence of Ca^{2+} for various times t_1, and finally

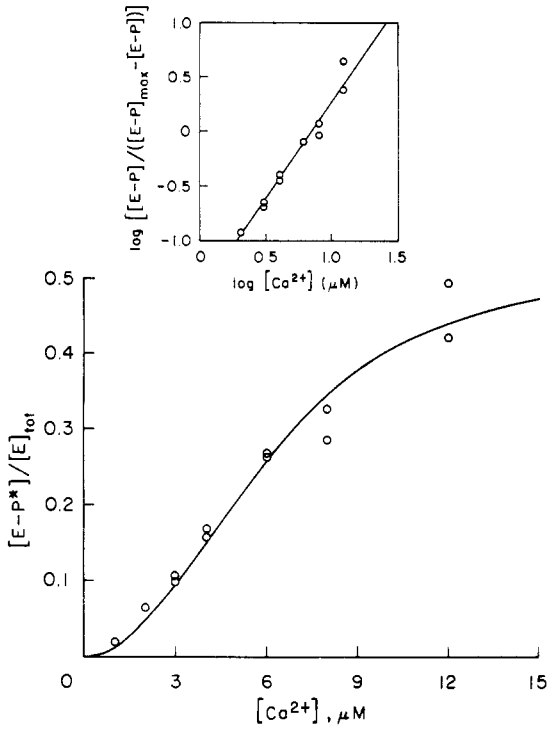

FIGURE 4: Dependence on $[Ca^{2+}]$ of E·ATP* trapping to give E~P*·Ca_2. With the four-syringe system, E was mixed with 15 μM [γ-^{32}P]ATP for t_1 = 100–120 ms and then reacted with various concentrations of Ca^{2+} in the presence of a chase of 0.5 mM nonradioactive ATP for $t_2 \geq 60$ ms. All syringes except D contained 40 mM MOPS (pH 7.0), 0.1 M KCl, and 5 mM $MgSO_4$. In addition, syringe A contained 0.13 mg/mL SRV passively loaded with 50 mM $CaCl_2$ and 2.0 mM EGTA; syringe B contained 30 μM [γ-^{32}P]ATP; syringe C contained 1.5 mM nonradioactive ATP, 19 mM EGTA, and either 0, 11.57, 14.83, 16.35, 17.23, 18.21, 18.75, 19.28, or 20.45 mM $CaCl_2$. This protocol was chosen in order to minimize the transiently high $[Ca^{2+}]$ that would result from mixing together a high concentration of free Ca^{2+} with EGTA since chelation is not instantaneous (Smith et al., 1977). For this mixing protocol, the initial Ca^{2+} concentration calculated to exist immediately upon mixing during t_2 for each point in the plot (the final $[Ca^{2+}]$ is shown in parentheses) is 0.37 μM (1.0 μM), 0.87 μM (2.0 μM), 1.5 μM (3.0 μM), 2.3 μM (4.0 μM), 5.6 μM (6.0 μM), 15.3 μM (8.0 μM), and 107 μM (12.0 μM). The amount of [^{32}P]E~P·Ca_2 trapped at each $[Ca^{2+}]$ was calculated as the fraction of $[E-P]_{max}$, the amount trapped in a run with 300 μM Ca^{2+} (not shown), which is plotted as $0.6[E_{tot}]$; the relative fractions trapped at lower $[Ca^{2+}]$ are adjusted accordingly. The solid line was calculated according to Scheme III (Materials and Methods). A Hill plot of the $[Ca^{2+}]$ dependence for the fraction of the maximum trapping of E·ATP is shown in the inset.

reacting with saturating Ca^{2+} for sufficient time to allow phosphorylation to proceed to completion.

Trapping of E·ATP·Ca_2. Figure 6 shows the observed formation of phosphoenzyme when passively loaded SRV are preincubated with EGTA for 15 s and then reacted with 300 μM [γ-^{32}P]ATP and 50 μM free Ca^{2+} for t_1 = 4.5 ms, followed by a chase of 5 mM EGTA during t_2 that lowers the concentration of free Ca^{2+} to 0.25 μM. The second-order rate constant of 2×10^6 M^{-1} s^{-1} for chelation of Ca^{2+} by EGTA (Smith et al., 1977) corresponds to a half-time of 0.1 ms for chelation by 5 mM EGTA. About 20% of the enzyme becomes labeled during t_1, and 20% of the remaining enzyme becomes labeled following the EGTA chase. A similar experiment in which the ATP was present during the 15-s preincubation to form E·ATP resulted in phosphorylation of 18% of the enzyme following the EGTA chase (data not shown). This shows that preincubation with ATP has no effect. The fact that the level of phosphoenzyme does not increase after 10 ms shows that the rate constant for phosphorylation of E·ATP* in the presence of 0.25 μM Ca^{2+} is insignificant.

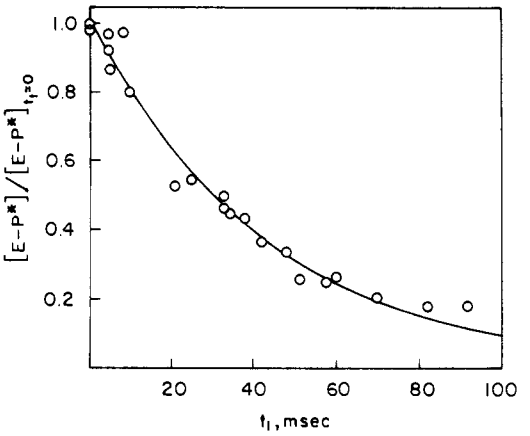

FIGURE 5: Measurement of the rate constant for the dissociation of E·ATP* (E·[γ-^{32}P]ATP). The rapid mix apparatus was used with four syringes. All syringes except D contained 40 mM MOPS (pH 7.0), 0.1 M KCl, and 5 mM $MgSO_4$. In addition, syringe A contained 5 mM EGTA, 15 μM [γ-^{32}P]ATP, and 0.13 mg/mL passively loaded SRV; syringe B contained 1 mM nonradioactive ATP; syringe C contained 5.9 mM $CaCl_2$. This provides a concentration of free Ca^{2+} of 300 μM during t_2. For the points at t_1 = 0, 5.6 mM $CaCl_2$ was added to syringe B, and syringe C contained only 0.3 mM $CaCl_2$. The plot shows the fraction of [^{32}P]E~P·Ca_2 (compared with t_1 = 0) that remains after various times t_1. The length of t_2 was ≥50 ms to allow phosphorylation (which has an observed rate constant of 117 s^{-1} in the presence of a nonradioactive chase, Figure 3) to reach completion. The line is drawn for a first-order rate constant of 24 s^{-1}.

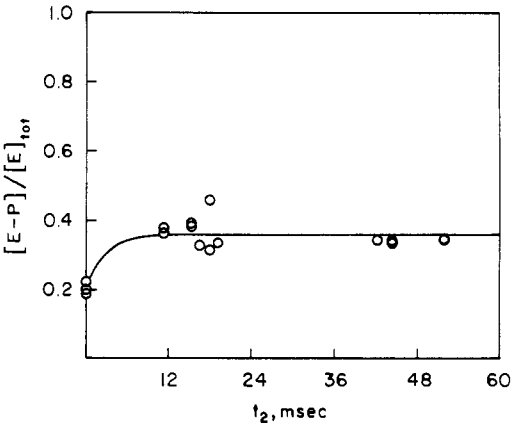

FIGURE 6: Phosphorylation of E·ATP·Ca_2 to give E~P·Ca_2 in the presence of an EGTA chase. With the four-syringe system, E was mixed with 50 μM Ca^{2+} and 300 μM [γ-^{32}P]ATP for t_1 = 4.5 ms and then chased with 5 mM EGTA for various times t_2 to lower the concentration of free Ca^{2+} to 0.25 μM. All syringes except D contained 40 mM MOPS (pH 7.0), 0.1 M KCl, and 5 mM $MgSO_4$. In addition, syringe A contained 0.61 mg/mL passively loaded SRV and 5 mM EGTA; syringe B contained 5.03 mM $CaCl_2$ and 600 μM [γ-^{32}P]ATP; syringe C contained 15 mM EGTA. t_1 was held constant at 4.5 ms, and the duration of t_2 was varied. The fraction of E_{tot} that is phosphorylated at t_2 = 0 was measured by reversing the order of addition from syringes C and D. The line is drawn for a first-order rate constant of 350 s^{-1} as described in the text, starting at 0.20 and with an end point of 0.20 + 0.17 = 0.37.

Dependence on $[Ca^{2+}]$ of the Reaction of E~P·Ca_2 with ADP. The reaction of [^{32}P]E~P·Ca_2 with 1.1 mM ADP in the presence of a nonradioactive ATP chase is biphasic, proceeding with a rapid burst of [^{32}P]E~P·Ca_2 disappearance followed by a slow phase (Figure 7; Sumida et al., 1980; Froehlich et al., 1980; Pickart & Jencks, 1982; Froehlich & Heller, 1985; Wang, 1986; Fernandez-Belda & Inesi, 1986). The size of the burst is independent of the concentration of Ca^{2+}, but the observed rate constant for phosphoenzyme disappearance in the slow phase increases 2.5-fold when the

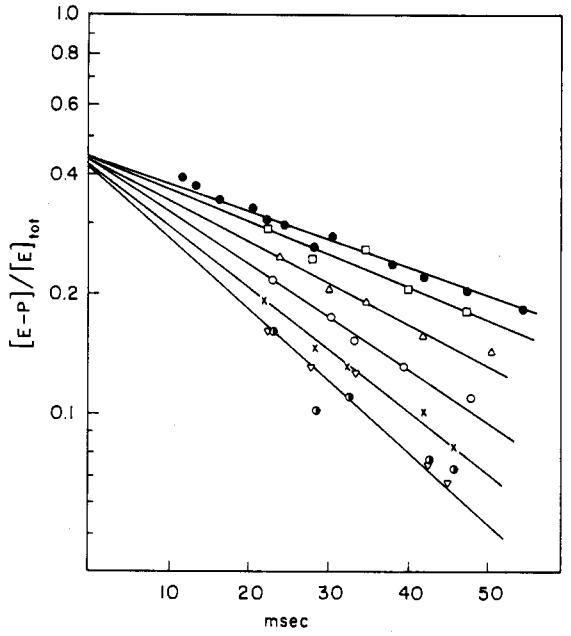

FIGURE 7: Effect of $[Ca^{2+}]$ on the reaction of $[^{32}P]E\sim P\cdot Ca_2$ with 1.1 mM ADP. $[^{32}P]E\sim P\cdot Ca_2$ was made by preincubating 0.29 mg/mL passively filled SRV with 10 μM $[\gamma\text{-}^{32}P]$ATP in 200 μM Ca^{2+} during the 15 s required to load the solution into the mixer. The reactions were carried out in the presence of 50 (●), 5 (□), 3 (△), 1 (○), 0.6 (×), 0.1 (▽), and 0.01 (◑) μM free Ca^{2+}. In addition to 40 mM MOPS (pH 7.0), 0.1 M KCl, and 5 mM $MgSO_4$, syringe A contained 10 μM $[\gamma\text{-}^{32}P]$ATP and passively filled SRV, and syringe B contained 15 mM EGTA and 14.8 (●), 13.0 (□), 11.9 (△), 8.5 (○), 6.6 (×), 1.7 (▽), or 0 (◑) mM $CaCl_2$.

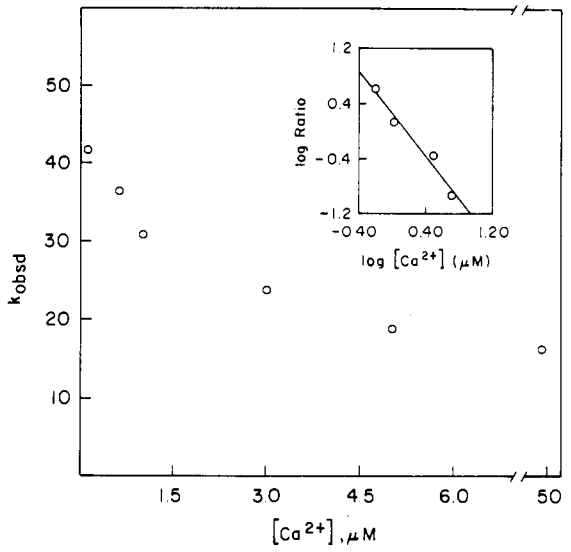

FIGURE 8: Effect of $[Ca^{2+}]$ on the rate constant of the slow phase for the reaction of $E\sim P\cdot Ca_2$ with 1.1 mM ADP (Figure 7). The Hill plot (inset) is based on the rate constant ratio $= (k - k_0)/(k_{max} - k)$, in which k_0 and k_{max} are the rate constants at 50 and 0.1 μM Ca^{2+}, respectively.

concentration of external Ca^{2+} is decreased from 50 μM to 10 nM (Figure 7; Pickart & Jencks, 1982). A plot of the rate constants for the slow phase at each Ca^{2+} concentration in Figure 7 shows a half-maximal increase at 1.7 μM Ca^{2+} (Figure 8). A Hill plot of these data has a slope of $n = 1.5$ (Figure 8, inset), but this value is not reliable because an error of only 2 s^{-1} in the values of the rate constants at 0.6 and 5 μM would result in a slope of 1.0 or 2.0.

Other Reactions. Attempts were made to measure the rate constants for hydrolysis of $E\sim P\cdot Ca_2$ with loaded vesicles and for phosphorylation of the enzyme in the absence of Ca^{2+}, in order to set limits for the specificities that are defined by the coupling rules for this enzyme. The experiments were carried out under standard conditions, except as indicated.

Scheme II′

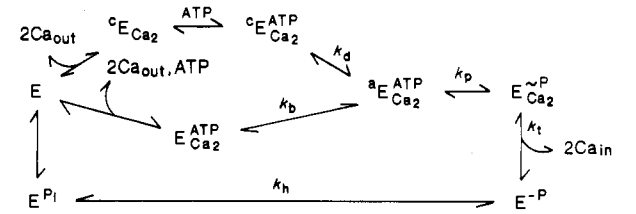

An upper limit of $k_{HOH} \leq 0.14$ s^{-1} was obtained for the hydrolysis of $E\sim P\cdot Ca_2$ from an observed half-time of 5 s for the disappearance of labeled phosphoenzyme that was obtained by manual quenching. Intact vesicles that had been passively loaded with 20 mM Ca^{2+} were phosphorylated with 15 μM $[\gamma\text{-}^{32}P]$ATP and 300 μM Ca^{2+} and then added to 0.5 mM unlabeled ATP (which had been incubated with phosphoenolpyruvate and pyruvate kinase to remove contaminating ADP).

An upper limit of $<6 \times 10^{-3}$ s^{-1} was obtained for the rate constant for phosphorylation of passively loaded vesicles in the absence of Ca^{2+} (preincubated with 5 mM EGTA for 15 s) in the presence of 15 μM $[\gamma\text{-}^{32}P]$ATP for 15 s. Identical radioactivity was found in vesicles that were quenched before and after the addition of $[\gamma\text{-}^{32}P]$ATP. The limit was calculated by assuming that 4% phosphorylation (2-fold over the blank) could be undetected in vesicles that hydrolyze $E\sim P\cdot Ca_2$ at 0.14 s^{-1}. The same result was obtained with 0, 5, and 50 mM $MgCl_2$. This shows that a high concentration of Mg^{2+} cannot substitute for Ca^{2+}. There is evidence that Mg^{2+} can bind to the Ca^{2+} site (Loomis & Tanford, 1982).

Discussion

The results reported here may be described by the model of Scheme II′. The principal difference between Scheme II′ and most models for the calcium ATPase is that in Scheme II′ there are two pathways for the reaction with ATP, the well-known pathway that involves a slow reaction of calcium with E to form the stable, high-affinity species $^cE\cdot Ca_2$, followed by binding of ATP and phosphorylation (top), and another that involves fast binding of ATP and calcium before phosphorylation (center). In both pathways the rate-limiting step for phosphorylation after ATP binds is a conformational change to form a catalytically active species of the enzyme, $^aE\cdot ATP\cdot Ca_2$, with a rate constant k_b or k_d, which is followed by very rapid phosphoryl transfer.

Binding of ATP to E. The results presented in Figure 1 show that the rate of phosphoenzyme formation when 200 μM ATP and Ca^{2+} are added simultaneously to free enzyme is close to that observed when E is preincubated with ATP, with $k_b = 70$ s^{-1} (Stahl & Jencks, 1984). Thus, if there is a conformational change upon ATP binding before the 70-s^{-1} step, it is extremely fast. The data can be fitted with a single rate constant of 62 s^{-1} (Figure 1, dotted line) or with two consecutive exponentials corresponding to rate constants of 1060 s^{-1} and 67 s^{-1} (solid line). The second-order rate constant for ATP binding to E is 5.3×10^6 M^{-1} s^{-1}, calculated from the dissociation constant of 4.5 μM (Stahl & Jencks, 1984) and the rate constant of 24 s^{-1} for dissociation of ATP from E·ATP (Figure 5; see below). This gives a first-order rate constant of 1060 s^{-1} for the binding of 200 μM ATP, which accounts for the barely noticeable lag in Figure 1 without invoking a slow conformational change of E or $E\cdot Ca_2$. Phosphorylation with 100 μM ATP gives a distinct lag of ~2 ms, as required

by this value of the second-order rate constant for ATP binding (data not shown). Larger lags at lower ATP concentrations have been observed previously by Inesi et al. (1980) and by Ogawa and Harafuji (1986) with bullfrog enzyme. There may be a fast conformational change associated with this second-order rate constant, because it is significantly smaller than the rate constant of 10^8–10^9 M^{-1} s^{-1} that is expected for a diffusion-controlled reaction.

These rate constants show that at ATP concentrations below 200 μM the binding of ATP is partially rate limiting for phosphorylation. A conservative lower limit for the first-order rate constant of a conformational change directly associated with ATP binding is $\geq$500 s^{-1}.

The similarity in the phosphorylation time course observed with and without ATP preincubation suggests that the reaction proceeds through the same pathway under both conditions.

The 70-s^{-1} Conformational Change. Figure 2 shows that the initial rate for phosphorylation of passively loaded SRV in the presence of 0.25 mM ADP and three different concentrations of [γ-^{32}P]ATP in the range 0.5–1.0 mM is slower than in the absence of ADP (dotted line), but the first-order rate constant of 77 s^{-1} is similar to that observed in the absence of ADP. This reaction is an approach to equilibrium (eq 2);

$$E{\cdot}ATP{\cdot}Ca_2 \underset{k_r}{\overset{k_f}{\rightleftharpoons}} \begin{cases} E{\sim}P{\cdot}Ca_2{\cdot}ADP \\ E{\sim}P{\cdot}Ca_2 + ADP \end{cases} \quad (2)$$

0.25 mM ADP reacts very rapidly with [^{32}P]E$\sim$P·Ca_2 to form [γ-^{32}P]ATP (Pickart & Jencks, 1982) and lowers the equilibrium concentration of [^{32}P]E$\sim$P·Ca_2 to approximately half of [E_{tot}] (Figure 2).

This rate constant is inconsistent with the rate constant of 140 s^{-1} that is expected for approach to equilibrium if the phosphorylation step itself were rate limiting. The initial rate of a reaction approaching equilibrium is the same as that for a reaction going to completion, but the half-time is shorter because the end point is reached sooner; the first-order rate constant for approach to equilibrium is equal to the sum of the first-order rate constants for the forward and reverse reactions (Frost & Pearson, 1953). With 50% phosphoenzyme at equilibrium, the forward and reverse rate constants are equal, and the observed rate constant is given by $k_{obsd} = k_f + k_r = 70 + 70 = 140$ s^{-1}. The reverse reaction is (pseudo) first-order because ADP binds and dissociates rapidly under these conditions (Pickart & Jencks, 1982, 1984). The absence of a detectable effect of three different concentrations of ATP on k_{obsd} shows that ADP does not decrease the rate constant significantly by competition with ATP.

We conclude that the observed rate constant for phosphorylation of $k_b = 70 \pm 7$ s^{-1} does not represent the phosphorylation step itself; instead, it represents a rate-limiting conformational change that converts the enzyme to an active form, ^{a}E·ATP·Ca_2, which undergoes very rapid phosphorylation (Scheme II′). The same conclusion was reached for the phosphorylation of ^{c}E·Ca_2 by ATP, which occurs after a rate-limiting conformational change with $k_d = 220$ s^{-1} (eq 1) (Petithory & Jencks, 1986). The observed rate constant is independent of ADP concentration in these reactions because all of the enzyme molecules must traverse the rate-limiting conformational change before undergoing rapid equilibration of phosphoryl transfer to reach the end point. The initial rate is slower in the presence of ADP because only about 50% of the enzyme molecules become phosphorylated in the rapid equilibrium step after the conformational change.

An essentially identical amount of phosphoenzyme (50%) was observed for the approach to equilibrium with 0.25 mM ADP and 0.8–1.2 mM ATP after preincubation of E with Ca^{2+} to form ^{c}E·Ca_2 (Petithory & Jencks, 1986). This is the expected result for the mechanism of Scheme II′ because the same equilibrium is reached regardless of whether the reaction begins with E or ^{c}E·Ca_2.

Scheme IV

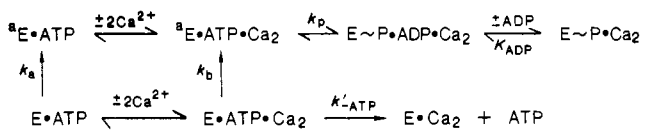

There are two conceivable pathways that could account for a rate-limiting conformational change preceding rapid phosphoryl transfer: the isomerization of E·ATP could occur at 70 s^{-1} before Ca^{2+} ions bind (k_a in Scheme IV), which would be consistent with the E_1–E_2 model (de Meis & Vianna, 1979; Inesi et al., 1980; Boyer & Ariki, 1980; Pick, 1981), or the conformational change could occur after the binding of two Ca^{2+} ions to the enzyme (k_b in Scheme IV). The following evidence shows that the 70-s^{-1} conformational change occurs after two Ca^{2+} ions bind to the enzyme.

Phosphorylation gives a yield of 55% phosphoenzyme with an observed rate constant of 117 s^{-1} when E is preincubated with [γ-^{32}P]ATP and an excess of nonradioactive ATP chase is added with the Ca^{2+} (Figure 3, lower line). This shows that the rate constants for the conformational change, k_b, and for the dissociation of ATP*, k'_{-ATP} in Scheme IV, are similar; i.e., the dissociation of ATP* is not in rapid equilibrium relative to phosphoryl transfer (Figure 3; Pickart & Jencks, 1982; Shigekawa & Kanazawa, 1982; Stahl & Jencks, 1984; Froehlich & Heller, 1985; Petithory & Jencks, 1986). The observed rate constant of 117 s^{-1} is the sum of $k_b = 70$ s^{-1} for phosphorylation and $k'_{-ATP} = 117 - 70 = 47$ s^{-1} for the dissociation of ATP*, which provides an additional pathway for the disappearance of the reacting E·ATP*·Ca_2 in the presence of a nonradioactive ATP chase. Dissociation of ATP* from intermediates formed after the rate-limiting conformational change would not cause an increase in the observed rate constant. The fraction of phosphorylation predicted by the rate constants is 70/117 = 0.60, which is close to the observed fraction of 0.55. Therefore, $\leq$5% of the labeled ATP dissociates after the conformational change.

The rate constant for the dissociation of ATP from E·ATP is 24 s^{-1} (Figure 5). The rate constant of $k'_{-ATP} = 47$ s^{-1} for the dissociation of ATP in the presence of Ca^{2+} shows that ATP is dissociating from a different species; i.e., it is dissociating from E·ATP·Ca_2 before the rate-limiting conformational change, k_b, and not from E·ATP before the k_a step (Scheme IV). Therefore, calcium must bind in order to permit the conformational change, which converts the enzyme to a catalytically active form that can react with bound ATP.

The results in Figure 6 show directly that Ca^{2+}-containing enzyme species accumulate *before* the 70-s^{-1} conformational change. Addition of an EGTA chase following a 4.5-ms pulse of 300 μM [γ-^{32}P]ATP and 50 μM Ca^{2+} results in the formation of [^{32}P]E$\sim$P·Ca_2 during the chase that corresponds to $\sim$20% of the enzyme that is unphosphorylated when EGTA is added. The observation that phosphorylation occurs in the presence of an EGTA chase shows that phosphorylation occurs through the k_b pathway after the binding to E·ATP of two Ca^{2+} ions to form E·ATP·Ca_2, which partitions between the rate-limiting conformational change (k_b) at 70 s^{-1} and dissociation of Ca^{2+}. Calcium-containing enzyme intermediates would not accumulate to any significant extent if phosphorylation proceeded through a rate-limiting conformational

Scheme V

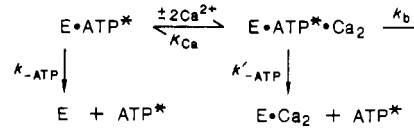

change before Ca^{2+} binding according to the k_a pathway of Scheme IV. The absence of biphasic kinetics in the phosphorylation time course at saturating [ATP] (Figure 3; Stahl & Jencks, 1984) indicates that all steps following the conformational change are fast; it also shows that calcium binding is fast and not kinetically significant under the conditions of these experiments. There is little Ca^{2+} dissociation after the k_b conformational change (see above).

All molecules of enzyme must have Ca^{2+} bound after 4.5 ms because no lags are observed for phosphorylation under these conditions and the observed rate constant for phosphorylation is independent of Ca^{2+} concentration above 50 μM (Stahl & Jencks, 1984). The observation that ~20% of the E·ATP·Ca_2 partitions toward phosphoenzyme formation indicates that 80% undergoes irreversible Ca^{2+} dissociation in the presence of the EGTA chase. Thus, the rate constant for the dissociation of Ca^{2+} is 280 s^{-1}, fourfold larger than k_b, and the overall rate constant for the disappearance of E·ATP·Ca_2 is ~280 + 70 = ~350 s^{-1}. These rate constants are too large to observe directly in the experiment of Figure 6.

Evidence will be described below that the species ^{a}E·ATP·Ca_2, which is formed in the k_b step, can also be formed from the reaction of E~P·Ca_2 with ADP and has different properties compared with E·ATP·Ca_2. This provides additional evidence that there must be a conformational change that interconverts these two species.

Ca^{2+} Binding Sites of E·ATP. The fraction of E·ATP* that is trapped with a chase of unlabeled ATP and Ca^{2+} decreases with decreasing Ca^{2+} concentration, giving half-maximal trapping at $K_{0.5}$ = 6.8 μM; the Hill slope is n = 1.8 (Figure 4). The value of $K_{0.5}$ is smaller than the equilibrium constant for dissociation of Ca^{2+} from E·ATP·Ca_2 because the rate constant that gives phosphorylation, k_b, is larger than that for ATP dissociation from E·ATP, k_{-ATP}. However, an estimate of this dissociation constant can be obtained from the model for trapping shown in Scheme V, assuming that Ca^{2+} binding is at equilibrium. The results of Figure 6 suggest that this assumption is a reasonable first approximation; the rate constant of 280 s^{-1} for Ca^{2+} dissociation is 4-fold larger than k_b = 70 s^{-1} for phosphorylation and more than twice $k_b + k'_{-ATP}$ = 117 s^{-1}. A second assumption is that an intermediate E·ATP*·Ca (with one Ca^{2+} ion bound) does not accumulate to a significant extent and that little ATP dissociation occurs from this intermediate. The fact that the Hill slope for the Ca^{2+} dependence of trapping is near 2 suggests that this assumption is valid.

With these assumptions, Scheme V shows that the fraction trapped at subsaturating concentrations of Ca^{2+} reflects the competition between dissociation of ATP, which is described by k_{-ATP}[E·ATP*] and k'_{-ATP}[E·ATP*·Ca_2], and phosphorylation, described by k_b[E·ATP*·Ca_2]. The dissociation constant for calcium, K_{Ca} (eq 3), was estimated from eq 4, which

$$K_{Ca} = \frac{[E\cdot ATP][Ca]^2}{[E\cdot ATP\cdot Ca_2]} \quad (3)$$

$$\frac{[E\sim P^*\cdot Ca_2]}{[E] + [E\cdot Ca_2]} = \frac{k_b[E\cdot ATP^*\cdot Ca_2]}{k_{-ATP}[E\cdot ATP^*] + k'_{-ATP}[E\cdot ATP^*\cdot Ca_2]} \quad (4)$$

gives a value of [E·ATP]/[E·ATP·Ca_2] = 4.85 from the ratio

Scheme VI

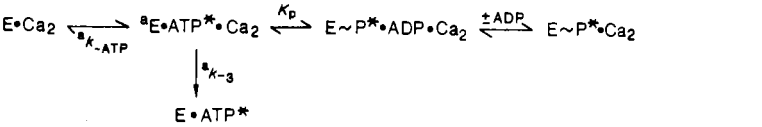

[E~P*·Ca_2]/([E] + [E·Ca_2]) = 0.3/0.7 at $K_{0.5}$ = 6.8 μM Ca^{2+} (Figure 4) and the observed values of k_b, k_{-ATP}, and k'_{-ATP}. The value of K_{Ca} = 2.2 × 10^{-10} M^2 corresponds to half-maximal saturation of Ca^{2+} binding to E·ATP at 15 μM Ca^{2+}. This binding is considerably weaker than the overall affinity of the enzyme for Ca^{2+}, which was calculated to be 5.9 × 10^{-12} M^2 ($K_{0.5}$ = 2.4 μM) in the absence of ATP under identical conditions (Pickart & Jencks, 1984). This shows that E·ATP differs from ^{c}E or "E_1", which have a much higher affinity for Ca^{2+}.

A nonlinear least-squares fit of the results in Figure 4 to an equation derived by the method of Cleland that describes trapping of E·ATP according to Scheme III, but does not assume that the binding of Ca^{2+} is at equilibrium (Materials and Methods), gave a result consistent with this value. Although no unique values of the rate constants for Ca^{2+} binding and dissociation resulted from this procedure, each solution set gave a value of K_{Ca} = 2.2 × 10^{-10} M^2 ($K_{0.5}$ = 15 μM Ca^{2+}). Fixing k_{-3} at 280 s^{-1} gave K_{Ca} = 1.7 × 10^{-10} M^2 ($K_{0.5}$ = 13 μM). Application of the same procedure to a model with stepwise dissociation of the two Ca^{2+} ions and dissociation of ATP also from the E·ATP·Ca intermediate gave K_{Ca} = 8 × 10^{-11} M^2 and $K_{0.5}$ = 9 μM Ca^{2+} (not shown).

Reaction of E~P·Ca_2 with ADP. A variety of models has been proposed to explain the biphasic reaction of E~P·Ca_2 with ADP, which proceeds with a rapid burst of phosphoenzyme disappearance followed by a slow phase (Sumida et al., 1980; Froehlich et al., 1980; Pickart & Jencks, 1982; Froehlich & Heller, 1985; Wang, 1986; Fernandez-Belda & Inesi, 1986). The biphasic reaction has been thought to represent two forms of Ca^{2+}-containing phosphoenzyme (E_1~P·Ca_2 and E_2–P·Ca_2) that differ in their sensitivity to ADP, as shown in Scheme I (Sumida et al., 1980; Froehlich et al., 1980). An alternative model is shown in Scheme VI, in which the burst of phosphoenzyme disappearance results from the equilibrium binding of ADP to [^{32}P]E~P·Ca_2 followed by rapid phosphoryl transfer to form enzyme-bound [γ-^{32}P]ATP, which dissociates slowly in the rate-limiting step of the slow phase (Pickart & Jencks, 1982; Fernandez-Belda & Inesi, 1986).

Although the reported yields vary, there is general agreement that most or all of E~P·Ca_2 is ADP-sensitive and gives ATP as the product under the conditions of these experiments [see also Kanazawa et al. (1971) and Nakamura et al. (1986)]; there is no clear evidence for the existence of a calcium-containing, ADP-insensitive phosphoenzyme, "E_2–P·Ca_2". The basic experimental features of the model in Scheme VI have received continued support (Froehlich & Heller, 1985; Wang, 1986), and the facts that ATP dissociation from the enzyme is slow (Pickart & Jencks, 1982; Shigekawa & Kanazawa, 1982; Stahl & Jencks, 1984; Froehlich & Heller, 1985; Petithory & Jencks, 1986; this work) and phosphoryl transfer to bound ADP is rapid and reversible (Pickart & Jencks, 1982) would appear to *require* that the mechanism shown in Scheme VI contribute to the observed result.

The mechanism of Scheme VI is further supported by the observation that the rate constant for the slow phase of the biphasic reaction of ADP with [^{32}P]E~P·Ca_2 increases with decreasing concentrations of Ca^{2+} on the outside of the vesicle,

Scheme VII

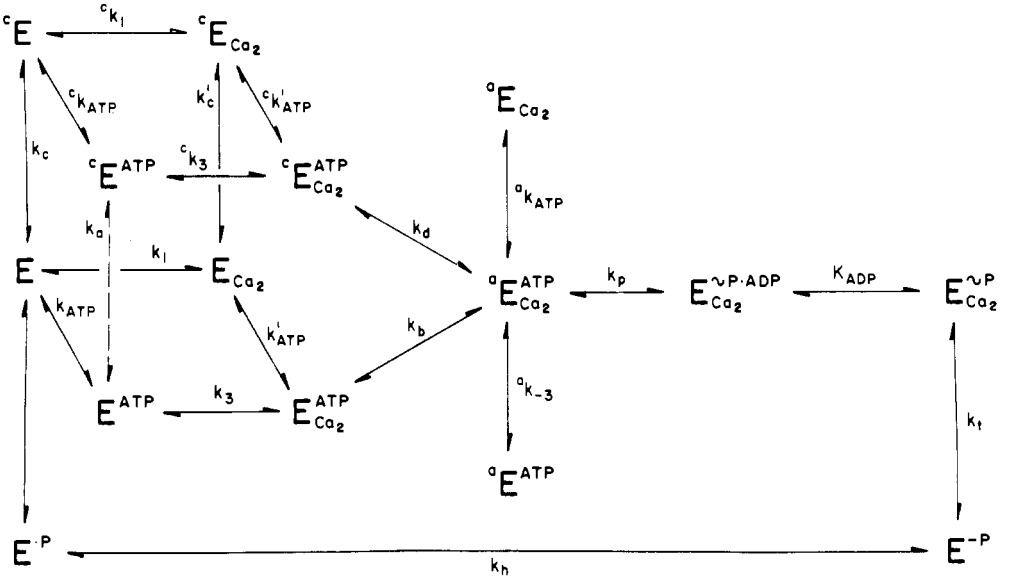

while the size of the burst remains approximately constant (Figure 7; Pickart & Jencks, 1982). Dissociation of Ca^{2+} ions from $^{a}E{\cdot}ATP^{*}{\cdot}Ca_2$ becomes irreversible in the limit of zero external $[Ca^{2+}]$ and gives an unreactive species that cannot form phosphoenzyme. It provides a new pathway for the disappearance of $^{a}E{\cdot}ATP^{*}{\cdot}Ca_2$, which accumulates before the rate-limiting dissociation of ATP*. According to Scheme VI, the apparent rate constant for the slow phase of $[^{32}P]E{\sim}P{\cdot}Ca_2$ disappearance increases by an amount equal to $^{a}k_{-3}$ for Ca^{2+} dissociation divided by the fraction of the enzyme that exists in the form $^{a}E{\cdot}ATP^{*}{\cdot}Ca_2$, which is given by the size of the burst in Figure 7. This corresponds to $^{a}k_{-3} = (42 - 17)/0.55 = 45\ s^{-1}$, from the results in Figure 7. This value agrees well with the previously reported rate constant of $\sim 50\ s^{-1}$ (Pickart & Jencks, 1982).

At intermediate concentrations of Ca^{2+}, enzyme species containing $[\gamma\text{-}^{32}P]ATP$ and zero or one Ca^{2+} ion will partition between dissociation of ATP and binding of Ca^{2+}, which allows reentry into the phosphoryl transfer equilibrium and results in smaller increases in the observed rate constant for the slow phase of the reaction. The dependence on $[Ca^{2+}]$ of the observed rate constant for the slow phase shows a half-maximal increase at 1.7 μM (Figure 8). The kinetics of this inhibition of Ca^{2+} dissociation are complex, and the value of $K_{0.5} = 1.7$ μM is not the equilibrium constant for the dissociation of Ca^{2+} from $^{a}E{\cdot}ATP^{*}{\cdot}Ca_2$. However, it does indicate that there is a high-affinity binding site for Ca^{2+} on $^{a}E{\cdot}ATP^{*}$. Furthermore, the value of $K_{0.5} = 1.7$ μM is certainly not equal to the value of $K_{0.5} = 6.8$ μM observed for the Ca^{2+} dependence of trapping E·ATP* (Figure 4). This difference confirms the conclusion that $E{\cdot}ATP{\cdot}Ca_2$ and $^{a}E{\cdot}ATP{\cdot}Ca_2$ are different species that are formed in different parts of the reaction pathway and may be interconverted by a conformational change.

These results are not easily explained by the classic E_1–E_2 model (Scheme I) or by more recent elaborations of this model (Froehlich & Heller, 1985; Wang, 1986). In these models, the slow phase of the reaction involves conformational transitions between various forms of phosphenzyme that contain bound Ca^{2+} ions, which are not expected to be sensitive to micromolar changes in the concentration of Ca^{2+} at the vesicle exterior.

On the other hand, Scheme VI does not explain the acceleration or elimination of the slow phase of phosphoenzyme decay that is observed if the external Ca^{2+} concentration is increased to the millimolar level when ADP is added (Froehlich & Heller, 1985). The explanation of this result is not known, but it is conceivable that high concentrations of calcium could cause this effect by replacing Mg^{2+} in the Mg·ATP site, which would inhibit rephosphorylation by ATP (Vianna, 1975), or by binding to a different site, such as a K^+ binding site.

Table II: Summary of Rate and Equilibrium Constants for the Reaction Steps of Scheme VII at pH 7.0, 0.1 M KCl, 5 mM $MgSO_4$, and 25 °C[a]

constant	value	ref
k_{ATP}	$5.3 \times 10^6\ M^{-1}\ s^{-1}$	*d*
k_{-ATP}	$24\ s^{-1}$	*d*
$K_{ATP} = k_{-ATP}/k_{ATP}$	4.5×10^{-6} M	*d*
k'_{-ATP}	$47\ s^{-1}$	*d*
k_b	$70\ s^{-1}$	*b, d*
k_{-3}	$280\ s^{-1}$	*d*
$K_{Ca} = k_{-3}/k_3$	$(0.8\text{–}2.2) \times 10^{-10}\ M^2$	*d*
k_p	$\geq 1000\ s^{-1}$	*c, d*
$^{a}k_{-3}$	$20\text{–}45\ s^{-1}$	*d*
$^{a}k_{-ATP}$	$\leq 37\ s^{-1}$	*e*
k_d	$220\ s^{-1}$	*c*
k_{-d}	$\leq 155\ s^{-1}$	*c*
$^{c}k'_{-ATP}$	$120\ s^{-1}$	*c*
$^{c}k_{-3}$	$80\ s^{-1}$	*c*
k_c	$11\text{–}40\ s^{-1}$	*f, g*
k_t	$17\ s^{-1}$	*h, i*
k_h	$70\ s^{-1}$	*c*

[a] Rate constants k_{-x} refer to the reverse of rate constants k_x in Scheme VII. [b] Stahl & Jencks, 1984. [c] Petithory & Jencks, 1986. [d] This work. [e] Pickart & Jencks, 1982. [f] Guillain et al., 1980. [g] Fernandez-Belda et al., 1984. [h] Pickart & Jencks, 1984. [i] Inesi et al., 1983.

A Model for the Calcium ATPase. Scheme VII and Table II show a minimal model and rate constants for the calcium ATPase of SRV that are consistent with the data presented here, as well as some other results obtained under similar conditions (Pickart & Jencks, 1982, 1984; Stahl & Jencks, 1984; Petithory & Jencks, 1986). Different conformations of the enzyme are indicated with a superscripted prefix: E is the stable form of the enzyme, $^{c}E{\cdot}Ca_2$ is the stable form of enzyme with two Ca^{2+} ions bound to the transport sites, and $^{a}E{\cdot}ATP{\cdot}Ca_2$ is a conformation that is activated for catalysis of reversible phosphorylation with ATP. Although evidence exists for additional enzyme conformational changes (see below), they are not kinetically significant to the mechanism and are

omitted from Scheme VII for simplicity. Important aspects of this model that differ from the classical E_1–E_2 model, as well as simulations that predict bent double-reciprocal plots and phosphorylation overshoots, are described below.

Activation of Ca^{2+} Binding by ATP. The rate constant of 70 ± 7 s^{-1} for phosphorylation that is observed upon addition of ATP and Ca^{2+} to free enzyme (Figure 1) is larger than rate constants in the range 11–40 s^{-1} that have been observed for the slow conformational change associated with Ca^{2+} binding to the enzyme in the absence of ATP under similar conditions (Sumida et al., 1978; Takisawa & Tonomura, 1978; Scofano et al., 1979; Inesi et al., 1980; Guillain et al., 1980, 1981; Fernandez-Belda et al., 1984; Pickart & Jencks, 1984; Stahl & Jencks, 1984). This activation results from ATP bound to the active site, and not a regulatory site, because preincubation of the enzyme with submicromolar concentrations of ATP gives a burst of phosphorylation that corresponds to the fraction of E·ATP that is predicted from the dissociation constant of E·ATP (Stahl & Jencks, 1984; Ogawa & Harafuji, 1986).

According to the E_1–E_2 model (and similar models), ATP facilitates calcium binding by facilitating a conformational change from E_2 to E_1, which has two high-affinity calcium sites on the cytoplasmic face of the vesicle and undergoes rapid phosphorylation upon calcium binding (Rauch et al., 1978; Boyer & Ariki, 1980; Inesi et al., 1980; Pick, 1981; Reynolds et al., 1985; Inesi, 1985). The results reported here are inconsistent with this mechanism or similar mechanisms that involve a single reaction pathway; instead, ATP increases the rate of calcium binding and provides a facile path for turnover by initiating a *different* reaction pathway for calcium binding and phosphorylation, as shown in eq 1 and Scheme VII. The following evidence supports the conclusion that phosphorylation of E in the presence of ATP and Ca^{2+} occurs through the E·ATP·Ca_2 pathway of Scheme VII, while phosphorylation of enzyme that has been preincubated with Ca^{2+} to form ^{c}E·Ca_2 occurs through the ^{c}E·ATP·Ca_2 pathway.

(1) The rate-limiting step for phosphorylation through the ^{c}E·Ca_2 (or "E_1·Ca_2") pathway is a conformational change of ^{c}E·ATP·Ca_2 with $k_d = 220$ s^{-1} (Petithory & Jencks, 1986), whereas in the other pathway phosphorylation is controlled by a conformational change of E·ATP·Ca_2 with $k_b = 70$ s^{-1}.

(2) In the ^{c}E·Ca_2 pathway the rate constants for dissociation from ^{c}E·ATP·Ca_2 are 80 s^{-1} for Ca^{2+} and 120 s^{-1} for ATP (Petithory & Jencks, 1986), whereas in the E + ATP pathway the corresponding rate constants for dissociation from E·ATP·Ca_2 are 280 s^{-1} for Ca^{2+} and 47 s^{-1} for ATP.

(3) Phosphorylation through the E + ATP pathway occurs with a first-order rate constant of 70 s^{-1}. If this pathway proceeded through the final part of the ^{c}E·Ca_2 pathway, it would proceed through the ^{c}E·ATP·Ca_2 intermediate, which gives phosphorylation with $k_d = 220$ s^{-1}. An additional step with a rate constant of 220 s^{-1} would give an easily detectable lag in the time course for phosphorylation in the E + ATP pathway, but no such lag is observed.

According to the E_1–E_2 model, ATP binds to E_1 with greater affinity than to E_2, resulting in an increase in the fraction of E_1 and exposure of Ca^{2+} binding sites on the outside, rather than the inside, of the vesicle. Activation is observed because Ca^{2+} ions bind rapidly to the high-affinity sites on E_1·ATP, followed by fast phosphorylation. Several results are difficult to reconcile with this model.

First, the reaction course of the ATP-activation pathway is first order, with $k_b = 70 \pm 7$ s^{-1}, regardless of whether the reaction is started by the addition of Ca^{2+} to E·ATP or by the addition of Ca^{2+} and ATP together to E. There is no evidence for an initial conformational change that increases the affinity for calcium. Indeed, the affinity of E·ATP for Ca^{2+} in the ATP pathway ($K_{0.5} = 15$ μM) is considerably lower than the overall affinity of the enzyme for Ca^{2+} after long equilibration ($K_{0.5} \simeq 2.5$ μM; Pickart & Jencks, 1984). There may be a conformational change with $k > 500$ s^{-1} upon binding of ATP, but it does not have the characteristics that are expected for a change to the ^{c}E or "E_1" conformation.

Second, in the E + ATP pathway Ca^{2+} binds to sites on the outside of intact vesicles before phosphorylation. The observation of phosphorylation following an EGTA chase (Figure 6) and the different rate constants for dissociation of ATP from E·ATP and E·ATP·Ca_2 show that the two Ca^{2+} ions bind *before* the rate-limiting conformational change.

There is no evidence that ATP has especially strong binding to the ^{c}E species, which would be required if ATP were to induce a change to this conformation. The binding of ATP to ^{c}E itself is difficult or impossible to measure directly (because ^{c}E does not accumulate at equilibrium), but the dissociation constant for ATP from ^{c}E·ATP·Ca_2 of 15 μM (Pickart & Jencks, 1984) is larger than the dissociation constant of 4.5 μM from E·ATP (Stahl & Jencks, 1984), and 6.3 μM Ca^{2+} decreases the affinity of SRV for ADPCP, the γ-methylene analogue of ATP, by 3-fold (Ogawa et al., 1986). The absence of a burst or biphasic kinetics for phosphorylation when Ca^{2+} is added to E·ATP shows that there is no detectable accumulation of a second ^{c}E or "E_1"-like conformation of the enzyme upon incubation with ATP.

We conclude that ATP and calcium can bind directly to cytoplasmic-facing sites on E and induce isomerization to the catalytically active form, ^{a}E·ATP·Ca_2, which undergoes phosphorylation at a rate that is too fast to measure with our techniques. This isomerization brings about the change in catalytic specificity that permits phosphorylation by ATP, according to one of the rules for coupled transport.

ATP is known to perturb other steps of the reaction cycle also, including the disappearance of E~P·Ca_2 and reactions that involve inorganic phosphate; however, it is not known how fast ATP dissociates from the different enzyme species that are involved in these reactions (de Meis & de Mello, 1973; Shigekawa & Dougherty, 1978; Coan et al., 1979; McIntosh & Boyer, 1983; Pickart & Jencks, 1984; Champeil & Guillain, 1986; Wakayashi et al., 1986).

E·ATP·Ca_2 Accumulates in the Steady State. A limiting value of $k_b = 70$ s^{-1} for the conformational change in the E + ATP pathway leads to the prediction that a significant fraction of the enzyme should be unphosphorylated during steady-state turnover at saturating concentrations of ATP and Ca^{2+} if turnover proceeds through this pathway. The slowest step in the catalytic cycle of the calcium ATPase under these conditions is associated with the release of Ca^{2+} from E~P·Ca_2 to the inside of the vesicle with an observed rate constant of $k_t = 17$ s^{-1} (Inesi et al., 1983; Pickart & Jencks, 1984). If no other steps in the cycle contribute to rate limitation, then ~20% of the total enzyme, E_{tot}, should accumulate as E·ATP·Ca_2 during turnover in the steady state according to eq 5 (Cleland, 1975). If the hydrolysis of E–P (k_h in Scheme VII) has a rate constant near 70 s^{-1} (Guillain et al., 1984), then it will also be partly rate limiting, and the amount of E·ATP·Ca_2 present in the steady state will be reduced to ~16%.

$$\frac{[\text{E·ATP·Ca}_2]}{[\text{E}_{tot}]} = \frac{1/70}{1/70 + 1/17} = 0.20 \qquad (5)$$

The results in Table I confirm this prediction, showing that addition of a calcium ionophore to permit turnover decreases the level of phosphoenzyme by 11–17% relative to that observed with intact, passively loaded SRV, in which the breakdown of E~P·Ca_2 is less than 2 s^{-1} because of trapping of E–P by internal Ca^{2+}.

This conclusion is important because it confirms a prediction about the distribution of enzyme forms in the steady state on the basis of measurements of rate constants for the first turnover of the enzyme. It supports the conclusion that turnover occurs through the E + ATP pathway and the implicit assumption, which is frequently made, that the properties of the enzyme measured on the first turnover are the same as the properties observed during subsequent turnovers. A similar decrease of 15% in the phosphoenzyme concentration under steady-state conditions, compared with the maximum level, has recently been observed for hydrolysis at pH 6 (Champeil & Guillain, 1986).

Phosphorylation Overshoots. The accumulation of an unphosphorylated form of the enzyme, E·ATP·Ca_2, during the steady state can qualitatively explain the overshoot of E~P·Ca_2 formation that has been observed during phosphorylation under certain experimental conditions (Froehlich & Taylor, 1976; Takisawa & Tonomura, 1978; Sumida et al., 1980). An overshoot is observed when ATP is reacted with enzyme preincubated with calcium, but only if the SRV have not been passively loaded with Ca^{2+}. An overshoot is not observed when Ca^{2+}-free E is mixed with Ca^{2+} and ATP simultaneously, regardless of whether the SRV have been loaded (Figure 1; Takisawa & Tonomura, 1978).

The model of eq 1 and Scheme VII predicts these experimental results according to the following mechanism. Phosphorylation of °E·Ca_2 at 220 s^{-1} in the presence of saturating ATP rapidly converts nearly all of the enzyme to E~P·Ca_2. This species then breaks down to E–P with a rate constant of 17 s^{-1} (Inesi et al., 1983; Pickart & Jencks, 1984), which is followed by hydrolysis to E with $k_h \geq 70$ s^{-1} if the vesicles are leaky (Guillain et al., 1984). Subsequent hydrolysis of ATP in the steady state occurs through the E and ATP cycle, not °E, under most conditions. The steady-state concentration of phosphoenzyme is then reduced by up to 11–17% from the maximum concentration because the conformational change with $k_b = 70$ s^{-1} is partly rate limiting. Thus, an overshoot of phosphoenzyme concentration is observed during the initial turnover, before the steady state is reached.

Figure 9 shows a computer simulation of the time course for phosphorylation of leaky vesicles with 250 and 20 μM ATP, starting with °E·Ca_2. An overshoot of the phosphoenzyme level is observed that is larger and decreases faster at the higher ATP concentration, in agreement with the results of Froehlich and Taylor (1976). The smaller overshoot at the lower ATP concentration is caused by the slower rate of phosphorylation. No overshoot is predicted or observed when ATP and Ca^{2+} are added to E that was not preincubated with Ca^{2+}. The rate constant of 84 s^{-1} for phosphorylation that is observed under these conditions (Results) is close to the predicted rate constant of 87 s^{-1} calculated from the sum of $k_b = 70$ s^{-1} and $k_t = 17$ s^{-1} for the phosphorylation of E and the disappearance of E–P·Ca_2, respectively, in the approach to the steady state (Hiromi, 1979). The initial rate of phosphorylation is the same as that with Ca^{2+}-loaded vesicles, but the approach to a lower level of phosphoenzyme in the steady state gives a shorter half-time and a larger rate constant.

Thus, when the reaction is initiated with enzyme preincubated with calcium, °E·Ca_2, the behavior of the enzyme in the steady state is different from that of °E·Ca_2 in the first turnover.

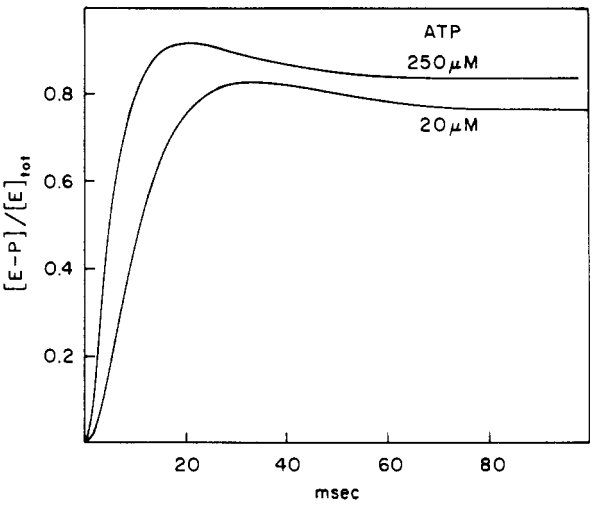

FIGURE 9: Simulation of the phosphorylation of °E·Ca_2 in leaky vesicles according to Scheme VII at saturating [Ca^{2+}]. A computer program described under Methods was used to simulate the time course of °E·Ca_2 with 250 or 20 μM ATP. The rate constants shown in Table II were used in the simulation, except that Ca^{2+} binding was assumed to be instantaneous. In the figure, E–P refers to the sum of the concentrations of all phosphorylated enzyme intermediates.

Simulation of Steady-State Kinetics. The existence of two reaction paths for phosphorylation also provides a plausible explanation for nonlinearity in Lineweaver–Burk plots for ATP hydrolysis in the low concentration range of ATP (Yamamoto & Tonomura, 1967; Inesi et al., 1967; Neet & Green, 1967; Vianna, 1975; Møller et al., 1980). At moderately high concentrations of ATP, steady-state hydrolysis proceeds through the ATP pathway with k_b partially rate limiting, as described above. However, at sufficiently low ATP concentration Ca^{2+} will bind to E to give °E·Ca_2 faster than phosphorylation occurs through the ATP pathway, so that the °E·Ca_2 pathway will be followed. This pathway has a relatively low maximal velocity because of the slow rate of formation of °E·Ca_2. This interpretation is consistent with previous suggestions that breaks in Lineweaver–Burk plots can be caused by a slow conformational change that is accelerated upon binding of a substrate (Smith et al., 1980; Moczydlowski & Fortes, 1981; Reynolds et al., 1985). However, it differs in that the increase in the rate of the conformational change arises from a different conformational change in a different reaction pathway, rather than from ATP-induced acceleration of a step in a single pathway.

Computer simulations of the mechanism of Scheme VII, as described under Methods, were found to give nonlinear double-reciprocal plots as a function of ATP concentration, in qualitative agreement with this conclusion (not shown). However, a quantitative treatment is not presented at this time because of uncertainty regarding the rate constants for the formation and reactions of °E·Ca_2.

Conformational Changes. One of the main features of the E_1–E_2 model is the existence of only two major conformations of the enzyme, E_1 and E_2, which differ with respect to the sidedness and affinity of their calcium sites as well as their chemical specificities for catalysis. A growing number of results indicate that this is an oversimplification; in fact, there may be conformational transitions associated with nearly every step in the catalytic cycle. It is perhaps not surprising that an enzyme that is designed to bring about coupled movement should undergo a number of conformational changes. Some of these conformational changes are outlined below.

(1) As described in this work, the isomerization of E·ATP·Ca_2 to ^{a}E·ATP·Ca_2, with $k_b = 70\ s^{-1}$, changes the catalytic specificity of the enzyme so that it reacts with ATP instead of phosphate. The rate constant for Ca^{2+} dissociation decreases from $k_{-3} = 280\ s^{-1}$ to $^ak_{-3} = 20$–$45\ s^{-1}$ (Scheme VII) as a result of this conformational change.

(2) The isomerization of ^{c}E·ATP·Ca_2 involves a rate-limiting conformational change of enzyme that has been preincubated with calcium, with $k_d = 220\ s^{-1}$. This step makes the enzyme competent for phosphorylation by ATP, the same change in catalytic specificity as the k_b step (Petithory & Jencks, 1986). It shows that occupancy of the high-affinity transport sites with Ca^{2+} is not sufficient to allow phosphorylation upon binding of ATP; a conformational transition following ATP binding is required before phosphoryl transfer can occur. This result is different from that predicted by the E_1–E_2 model, in which conversion of the enzyme to the E_1 form is necessary and sufficient to give phosphorylation upon binding of Ca^{2+} and ATP.

(3) Binding of Ca^{2+} to E to give ^{c}E·Ca_2 with a rate constant in the range 11–40 s^{-1} is widely believed to involve a rate-limiting conformational change, which is manifested by changes in fluorescence and other properties of the enzyme as well as a change in the rate constant for isomerization to ^{a}E·ATP·Ca_2 in the presence of ATP (Dupont & Leigh, 1978; Inesi et al., 1980; Guillain et al., 1980; Fernandez-Belda et al., 1984; Martonosi & Beeler, 1985; Highsmith, 1986).

(4) The release of Ca^{2+} to the inside of the vesicle from low-affinity sites on E~P·Ca_2 to give E–P, with $k_t = 17\ s^{-1}$, is the predominant rate-limiting step for turnover with saturating ATP and Ca^{2+}. It probably represents a conformational change because of its slow rate and because it involves the release of calcium and a change in catalytic specificity. It is also accompanied by a slow change in fluorescence (Dupont, 1978).

(5) Although there is no evidence for a slow conformational change associated with the binding of ATP to E, physical evidence and the low value of the second-order rate constant for ATP binding, $k_{ATP} = 5.3 \times 10^6\ M^{-1}\ s^{-1}$, suggest that an isomerization occurs that is too fast to detect. Upon binding of ATP there is an increase in the intrinsic protein fluorescence (Dupont et al., 1982; Fernandez-Belda et al., 1984), a change in the EPR signal of a covalently bound spin-labeled probe (Inesi et al., 1980), an increase in the rate of inactivation of ATPase activity by DCCD modification of an enzyme carboxylate group(s) that is (are) thought to be located at the Ca^{2+} binding site (Murphy, 1981), and a decrease in the chemical reactivity of thiol groups (Murphy, 1978).

(6) It is plausible, but not proved, that a conformational change upon binding of one Ca^{2+} ion to E·ATP·Ca to give E·ATP·Ca_2 accounts for the cooperativity of Ca^{2+} binding (Figure 4; Tanford, 1984) and for the ability to change catalytic specificity by isomerization to ^{a}E·ATP·Ca_2, with $k_b = 70\ s^{-1}$. However, the absence of a detectable lag in the phosphorylation time course requires that any such conformational change must have a rate constant of $>500\ s^{-1}$ (Figure 3; Stahl & Jencks, 1984).

(7) The small second-order rate constant of $5 \times 10^3\ M^{-1}\ s^{-1}$ for binding of P_i or Mg^{2+} to E (pH 6.0, [KCl] = 0, and 23 °C) is consistent with the suggestion that this binding involves a conformational change (Guillain et al., 1984). The formation of E–P·Mg from E involves a change in vectorial specificity that permits productive binding of Ca^{2+} to the phosphoenzyme from inside the vesicle. This change in the exposure of the calcium binding sites from outside to inside must almost certainly involve a conformational change.

Scheme VIII

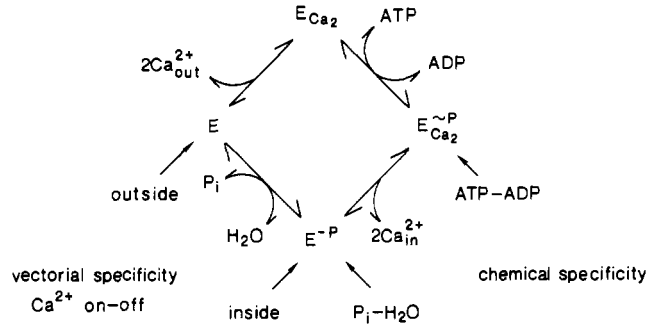

(8) The phosphorylation of ^{a}E·ATP·Ca_2 to give E~P·Ca_2 changes the direction from which calcium can dissociate, from the outside to the inside of the vesicle. This is the critical vectorial step for the active transport of calcium, and it must almost certainly involve a conformational change. Surprisingly, it occurs with a rate constant of $>1000\ s^{-1}$, which is too fast to measure with presently available techniques (Stahl & Jencks, 1984; Petithory & Jencks, 1986).

Coupling. The coupling of vectorial Ca^{2+} transport to ATP hydrolysis results from changes in the catalytic and vectorial specificities of different enzyme states. A simple set of specificity rules that describe coupling may be taken from experimentally observed properties of the calcium ATPase (Jencks, 1983). These rules represent changes in chemical specificity for catalysis and in vectorial specificity for calcium binding in different states of the enzyme, as outlined in Scheme VIII.

(1) The enzyme catalyzes reversible phosphorylation by ATP, not P_i, when Ca^{2+} is bound to the transport sites. (2) The enzyme catalyzes reversible phosphorylation by P_i, not ATP, when the transport sites are not occupied by Ca^{2+}. (3) Productive binding and release of Ca^{2+} occur only on the cytoplasmic side of the membrane when the enzyme is unphosphorylated. (4) Productive binding and release of Ca^{2+} occur only on the inside of the membrane when the enzyme is phosphorylated. Thus, Ca^{2+} binding acts as a catalytic switch that changes the catalytic specificity of the enzyme from P_i to ATP by facilitating an enzyme conformational change following the binding of ATP, while phosphorylation acts as a vectorial switch that changes the orientation of Ca^{2+} binding and dissociation from cytoplasmic (outside) to inside the vesicle. Violation of any of these rules results in uncoupling of Ca^{2+} transport from ATP hydrolysis; there is no one step in which coupling can be said to occur. The rules describe a strictly ordered kinetic mechanism with alternating chemical and vectorial steps. The cleavage of ATP and the transport of calcium are each divided into two parts that are sandwiched between the parts of the other process, so that neither the chemical nor the vectorial reaction can occur without the other.

Our results provide further support for the hypothesis that phosphorylation is the switch that determines on which side of the membrane Ca^{2+} binds and dissociates. We have concluded that the net rate constant for Ca^{2+} dissociation from ^{a}E·ATP·Ca_2 has a value of $45\ s^{-1}$. According to Scheme VII, there are three possible pathways through which Ca^{2+} can dissociate from this intermediate: (1) direct dissociation from ^{a}E·ATP·Ca_2 through the $^ak_{-3}$ step, (2) reversal of the k_d conformational change to give ^{c}E·ATP·Ca_2, and (3) reversal of the k_b conformational change, to give E·ATP·Ca_2. The observation that the increase in the net rate constant for Ca^{2+} dissociation is half-maximal at 1.7 μM Ca^{2+} (Figure 4) shows that little if any of the dissociation occurs through (3) because trapping of E·ATP·Ca_2 is half-maximal at 6.8 μM Ca^{2+}. The Ca^{2+} dissociation cannot be accounted for by (2) because the

ratio of the rate constants for dissociation of Ca^{2+} and ATP is 45/37 = 1.2 from $^{a}E{\cdot}ATP{\cdot}Ca_2$ and 80/120 = 0.67 from $^{c}E{\cdot}ATP{\cdot}Ca_2$ (this work; Pickart & Jencks, 1982; Petithory & Jencks, 1986). Furthermore, dissociation of Ca^{2+} from $^{c}E{\cdot}ATP{\cdot}Ca_2$ would require a rate constant of $k_{-d} = 310\ s^{-1}$ along with the measured value for $^{c}k_{-3} = 80\ s^{-1}$ (Petithory & Jencks, 1986) in order to account for a net rate constant of 45 s^{-1} for Ca^{2+} dissociation through pathway (2). The reverse rate constant k_{-d} is smaller than the forward rate constant k_d = 220 s^{-1} because $^{c}E{\cdot}ATP{\cdot}Ca_2$ is observed to form $^{a}E{\cdot}ATP{\cdot}Ca_2$, with a rate constant of $k_d = 220\ s^{-1}$ in the absence of ADP and 270 s^{-1} in the presence of ADP (Petithory & Jencks, 1986).

We conclude that some or all of the Ca^{2+} must dissociate directly from $^{a}E{\cdot}ATP{\cdot}Ca_2$. Even if all of the ATP dissociation were to occur through $^{c}E{\cdot}ATP{\cdot}Ca_2$, this would account for only $80/120 \times 37\ s^{-1} = 25\ s^{-1}$ for Ca^{2+} dissociation, so the Ca^{2+} must dissociate directly from $^{a}E{\cdot}ATP{\cdot}Ca_2$ with $^{a}k_{-3} \geq 20\ s^{-1}$. Thus, the phosphorylation step itself, with $k_p \geq 1000\ s^{-1}$, appears to be the critical vectorial step after which Ca^{2+} dissociation to the outside is forbidden and dissociation to the inside becomes possible.

Coupling of the transport of two Ca^{2+} ions to the hydrolysis of one molecule of ATP is remarkably strong; the Ca^{2+} concentration gradient that accumulates at different ratios of ATP and ADP is experimentally indistinguishable from that predicted from the Gibbs energy of ATP hydrolysis (Trevorrow & Haynes, 1984). Our kinetic analysis of the extent to which an enzyme intermediate reacts in a manner that violates a coupling rule agrees with this conclusion. For example, the direct hydrolysis of $E{\sim}P{\cdot}Ca_2$ violates the rule which states that the reaction of phosphoenzyme with water may occur only when Ca^{2+} is not bound; it results in uncoupled hydrolysis of ATP. The upper limit of $\leq 0.14\ s^{-1}$ (Results) for this hydrolysis gives uncoupling of <1% compared with the rate constant of 17 s^{-1} for turnover of $E{\sim}P{\cdot}Ca_2$ (Inesi et al., 1983; Pickart & Jencks, 1984) and is $\sim 10^4$ smaller than the rate constant of >1000 s^{-1} for the reaction of $E{\sim}P{\cdot}Ca_2$ with ADP (Petithory & Jencks, 1986).

Phosphorylation of the enzyme by ATP in the absence of calcium to give E–P violates the other specificity rule and would also give uncoupled hydrolysis of ATP, because E–P reacts rapidly with water. The upper limit of $< 6 \times 10^{-3}\ s^{-1}$ for this reaction is slower than turnover by a factor of $>10^3$ and is smaller than the rate constant for phosphorylation of $^{c}E{\cdot}ATP{\cdot}Ca_2$ by a factor of $>10^5$. The same limits hold for violation of the coupling rule that forbids productive binding of calcium to E from inside the loaded vesicle to give $^{c}E{\cdot}Ca_2$, because such binding would result in phosphorylation of the enzyme by ATP.

The Mg^{2+} ion is a competitive inhibitor for calcium binding to the ATPase (Kanazawa et al., 1971; Vianna, 1975), and the formation of phosphoenzyme from enzyme and inorganic phosphate at equilibrium is inhibited by high concentrations of Mg^{2+}. It has been suggested that this is the result of occupancy of the Ca^{2+} site by two Mg^{2+} ions, which destabilize the phosphoenzyme (Loomis & Tanford, 1982). The absence of any detectable phosphorylation by ATP in the presence of 50 mM Mg^{2+} shows that Mg^{2+} cannot substitute for Ca^{2+} in activating the enzyme for reaction with ATP. This suggests that occupancy of this site by divalent cations is insufficient to cause a detectable change in specificity for catalysis; i.e., small changes in geometry cause large changes in catalytic specificity. It is of interest that the specificity rule does appear to be violated in the presence of high concentrations of dimethyl sulfoxide, which induce a slow ATPase activity in the absence of Ca^{2+} (de Meis & Inesi, 1985).

A specificity factor of >50 can be set for the coupling rule that forbids calcium dissociation to the outside from $E{\sim}P{\cdot}Ca_2$ because such dissociation would give ATPase activity with intact vesicles in the absence of a calcium ionophore, which is typically <2% of the activity in the presence of ionophore. The actual factor is probably considerably larger than this because this ATPase activity may be caused by other enzymes and by leakage of calcium from the vesicle through other routes.

Low-Affinity Calcium Site of E. The observed rate constant of 84 s^{-1} for phosphorylation of leaky SRV upon addition of 100 μM Ca^{2+} to vesicles preincubated with 200 μM ATP is close to the value of 87 s^{-1} predicted for approach to the steady state with rate constants of 70 s^{-1} for phosphorylation (k_b) and 17 s^{-1} for breakdown of $E{\sim}P{\cdot}Ca_2$ (Hiromi, 1979). This result shows that there is no significant effect on k_b, the rate constant for the conformational change, of occupancy of the low-affinity Ca^{2+} binding sites exposed to the inside of vesicles that are passively loaded with 20 mM Ca^{2+} (Prager et al., 1979; Suko et al., 1981). Incubation in alkaline solution in the presence of EGTA to make the vesicles leaky also has no measurable effect on these rate constants.

ACKNOWLEDGMENTS

We are grateful to Joanne Petithory for contributing some of the data in Figure 2 and for stimulating discussion of the model in Scheme VII.

REFERENCES

Allen, D. G., Blinks, J. R., & Prendergast, F. G. (1977) *Science (Washington, D.C.) 195*, 996–998.

Barman, T. E., & Gutfreund, H. (1964) in *Rapid Mixing and Sampling Techniques in Biochemistry* (Chance, B., Eisenhardt, R. H., Gibson, Q. H., & Lonberg-Holm, K. K., Eds.) pp 339–344, Academic, New York.

Boyer, P. D., & Ariki, M. (1980) *Fed. Proc., Fed. Am. Soc. Exp. Biol. 39*, 2410–2414.

Champeil, P., & Guillain, F. (1986) *Biochemistry 25*, 7623–7633.

Cleland, W. W. (1975) *Biochemistry 14*, 3220–3224.

Coan, C., Verjovski-Almeida, S., & Inesi, G. (1979) *J. Biol. Chem. 254*, 2968–2974.

de Meis, L., & de Mello, M. C. F. (1973) *J. Biol. Chem. 248*, 3691–3701.

de Meis, L., & Vianna, A. L. (1979) *Annu. Rev. Biochem. 48*, 275–292.

de Meis, L., & Inesi, G. (1985) *Biochemistry 24*, 922.

Dupont, Y. (1978) *Biochem. Biophys. Res. Commun. 82*, 893–900.

Dupont, Y., & Leigh, J. B. (1978) *Nature (London) 273*, 396–398.

Dupont, Y., Bennett, N., & Lacapère, J.-J. (1982) *Ann. N.Y. Acad. Sci. 402*, 569–572.

Fernandez-Belda, F., & Inesi, G. (1986) *Biochemistry 25*, 8083–8089.

Fernandez-Belda, F., Kurzmack, M., & Inesi, G. (1984) *J. Biol. Chem. 259*, 9687–9698.

Froehlich, J. P., & Taylor, E. W. (1976) *J. Biol. Chem. 251*, 2307–2315.

Froehlich, J. P., & Heller, P. F. (1985) *Biochemistry 24*, 126–136.

Froehlich, J. P., Heller, P. F., & Passonneau, J. V. (1980) *Fed. Proc., Fed. Am. Soc. Exp. Biol. 39*, 2151.

Frost, A. A., & Pearson, R. G. (1953) *Kinetics and Mechanism*, pp 154–173, Wiley, New York.

Glynn, I. M., & Karlish, S. J. D. (1975) *Annu. Rev. Physiol. 37*, 13–55.
Godt, R. E. (1974) *J. Gen. Physiol. 63*, 722–739.
Guillain, F., Gingold, M. P., Büschlen, S., & Champeil, P. (1980) *J. Biol. Chem. 255*, 2072–2076.
Guillain, F., Champeil, P., Lacapère, J.-J., & Gingold, M. P. (1981) *J. Biol. Chem. 256*, 6140–6147.
Guillain, F., Champeil, P., & Boyer, P. D. (1984) *Biochemistry 23*, 4754–4761.
Highsmith, S. (1986) *Biochemistry 25*, 1049–1054.
Hiromi, K. (1979) *Kinetics of Fast Enzyme Reactions*, pp 220–223, Wiley, New York.
Inesi, G. (1985) *Annu. Rev. Physiol. 47*, 573–601.
Inesi, G., Goodman, J. J., & Watanabe, S. (1967) *J. Biol. Chem. 242*, 4637–4643.
Inesi, G., Kurzmack, M., Coan, C., & Lewis, D. E. (1980) *J. Biol. Chem. 255*, 3025–3031.
Inesi, G., Nakamoto, R., Hymel, L., & Fleischer, S. (1983) *J. Biol. Chem. 258*, 14804–14809.
Jencks, W. P. (1983) *Curr. Top. Membr. Transp. 19*, 1–19.
Kanazawa, T., Yamada, S., Yamamoto, T., & Tonomura, Y. (1971) *J. Biochem. (Tokyo) 70*, 95–123.
Loomis, C. R., Martin, D. W., McCaslin, D. R., & Tanford, C. (1982) *Biochemistry 21*, 151–156.
Lowry, O. H., Rosebrough, N. J., Farr, A. L., & Randall, R. J. (1951) *J. Biol. Chem. 193*, 265–275.
Martonosi, A. N., & Beeler, T. J. (1985) in *Handbook of Physiology* (Peachy, L. D., & Adrian, R. H., Eds.) Section 10, pp 417–485, American Physiological Society, Bethesda, MD.
McIntosh, D. B., & Boyer, P. D. (1983) *Biochemistry 22*, 2867–2875.
Moczydlowski, E. G., & Fortes, P. A. G. (1981) *J. Biol. Chem. 256*, 2357–2366.
Møller, J. V., Lind, K. E., & Anderson, J. P. (1980) *J. Biol. Chem. 255*, 1912–1920.
Murphy, A. J. (1978) *J. Biol. Chem. 253*, 385–389.
Murphy, A. J. (1981) *J. Biol. Chem. 256*, 12046–12050.
Nakamura, Y., Kurzmack, M., & Inesi, G. (1986) *J. Biol. Chem. 261*, 3090–3097.
Neet, K. E., & Green, N. M. (1977) *Arch. Biochem. Biophys. 178*, 588–597.
Ogawa, Y. (1968) *J. Biochem. (Tokyo) 64*, 255–257.
Ogawa, Y., & Harafuji, H. (1986) *J. Biochem. (Tokyo) 100*, 1319–1328.
Ogawa, Y., Kurebayashi, N., & Harafuji, H. (1986) *J. Biochem. (Tokyo) 100*, 1305–1318.
Petithory, J. R., & Jencks, W. P. (1986) *Biochemistry 25*, 4493–4497.
Pick, U. (1981) *Eur. J. Biochem. 121*, 187–195.
Pickart, C. M., & Jencks, W. P. (1982) *J. Biol. Chem. 257*, 5319–5322.
Pickart, C. M., & Jencks, W. P. (1984) *J. Biol. Chem. 259*, 1629–1643.
Post, R. L., Kume, W., Tobin, T., Orcutt, B., & Sen, A. K. (1969) *J. Gen. Physiol. 54*, 306s–326s.
Prager, R., Punzengruber, C., Kolassa, N., Winkler, F., & Suko, J. (1979) *Eur. J. Biochem. 97*, 239–250.
Rauch, B., von Chak, D., & Hasselbach, W. (1978) *FEBS Lett. 93*, 65–68.
Reynolds, J. A., Johnson, E. A., & Tanford, C. (1985) *Proc. Natl. Acad. Sci. U.S.A. 82*, 3658–3661.
Rossi, B., Leone, F. de A., Gache, C., & Lazdunski, M. (1979) *J. Biol. Chem. 254*, 2302–2307.
Schwarzenbach, G., Senn, H., & Anderegg, G. (1957) *Helv. Chim. Acta 40*, 1886–1900.
Scofano, H. M., Vieyra, A., & de Meis, L. (1979) *J. Biol. Chem. 254*, 10227–10231.
Seigel, G. J., & Albers, R. W. (1967) *J. Biol. Chem. 242*, 4972–4979.
Shigekawa, M., & Dougherty, J. P. (1978) *J. Biol. Chem. 253*, 1451–1457.
Shigekawa, M., & Kanazawa, T. (1982) *J. Biol. Chem. 257*, 7657–7665.
Smith, P. D., Berger, R. L., Podolsky, R. J., & Czerlinski, G. (1977) *Biophys. J. 17*, 159a.
Smith, R. L., Zinn, K., & Cantley, L. C. (1980) *J. Biol. Chem. 255*, 9852–9859.
Stahl, N., & Jencks, W. P. (1984) *Biochemistry 23*, 5389–5392.
Suko, J., Plank, B., Preis, P., Kolassa, N., Hellmann, G., & Conca, W. (1981) *Eur. J. Biochem. 119*, 225–236.
Sumida, M., Wang, T., Mandel, F., Froehlich, J. P., & Schwartz, A. (1978) *J. Biol. Chem. 253*, 8772–8777.
Sumida, M., Wang, T., Schwartz, A., Younkin, C., & Froehlich, J. P. (1980) *J. Biol. Chem. 255*, 1497–1503.
Takisawa, H., & Tonomura, Y. (1978) *J. Biochem. (Tokyo) 83*, 1275–1284.
Tanford, C. (1981) *J. Gen. Physiol. 77*, 223–229.
Tanford, C. (1984) *CRC Crit. Rev. Biochem. 17*, 123–151.
Tanford, C., Reynolds, J. A., & Johnson, E. A. (1985) *Proc. Natl. Acad. Sci. U.S.A. 82*, 4688–4692.
Trevorrow, K., & Haynes, D. H. (1984) *J. Bioenerg. Biomembr. 16*, 53–59.
Veech, R. L., Lawson, J. W. R., Cornell, N. W., & Krebs, H. A. (1979) *J. Biol. Chem. 254*, 6538–6547.
Verjovski-Almeida, S., Kurzmack, M., & Inesi, G. (1978) *Biochemistry 17*, 5006–5013.
Vianna, A. L. (1975) *Biochim. Biophys. Acta 410*, 389–406.
Wakabayashi, S., Ogurusu, T., & Shigekawa, M. (1986) *J. Biol. Chem. 261*, 9762–9769.
Wang, T. (1986) *J. Biol. Chem. 261*, 6307–6316.
Yamamoto, T., & Tonomura, Y. (1967) *J. Biochem. (Tokyo) 62*, 558–575.